

# Macroscopic Treatment of Radio Emission from Cosmic Ray Air Showers based on Shower Simulations

Klaus WERNER

*SUBATECH, Université de Nantes – IN2P3/CNRS – EMN, Nantes, France*

Olaf SCHOLTEN

*Kernfysisch Versneller Instituut, University of Groningen, 9747 AA, Groningen, The Netherlands*

We present a macroscopic calculation of coherent electro-magnetic radiation from air showers initiated by ultra-high energy cosmic rays, based on currents obtained from Monte Carlo simulations of air showers in a realistic geo-magnetic field. We can clearly relate the time signal to the time dependence of the currents. We find that the the most important contribution to the pulse is related to the time variation of the currents. For showers forming a sufficiently large angle with the magnetic field, the contribution due to the currents induced by the geo-magnetic field is dominant, but neither the charge excess nor the dipole contribution can be neglected. We find a characteristic bipolar signal. In our calculations, we take into account a realistic index of refraction, whose importance depends on the impact parameter and the inclination. Also very important is the role of the positive ions.

## I. INTRODUCTION

The main motivation for this work is the apparent need of radio detection experiments (LOPES [1, 2], CODALEMA [3]) for reliable calculations. Already in the earliest works on radio emission from air showers [4, 5, 6, 7], a macroscopic treatment of the radio emission was proposed, but at the time the assumptions about the currents were rather crude. In more recent work [8, 9, 10, 11, 12], a microscopic picture of coherent synchrotron radiation from secondary shower electrons and positrons gyrating in the Earth's magnetic field was employed.

Recently, we performed macroscopic calculations, which allow one under simplifying conditions to obtain a simple analytic expression for the pulse shape, showing a clear relation between the pulse shape and the shower profile [13]. The picture used was very similar to the one in Ref. [5], which has been refined by using a more realistic shower profile and where we calculate the time-dependence of the pulse.

In the present paper, we advance further by computing first the four-current from a realistic Monte Carlo simulation (in the presence of a geo-magnetic field), and then solve the Maxwell equations to obtain the electric field, while considering a realistic (variable) index of refraction. Although this index varies only between 1 and 1.0003, this variation has quite interesting consequences.

For the moment, we neglect the finite extension of the shower (pancake thickness and lateral extension), at a given time. As shown in [13], this is a good approximation for large impact parameters; for smaller ones the finite extension has to be considered. There are no conceptual problems in extending the present approach to finite size sources, which is simply a three-dimensional integral over the point-

like expressions. This will be discussed in a future publication.

The shower moves with almost the vacuum velocity of light  $c$ . There is a constant creation of electrons and positrons at the shower front, with somewhat more electrons than positrons (electron excess). This is compensated by positive ions in the air, essentially at rest. The electrons and positrons of the shower scatter and lose energy, and therefore they move slower than the shower front, falling behind, and finally drop out as “slow electrons / positrons”. Close to the shower maximum, the charge excess of the “dropping out” particles is compensated by the positive ions, since there is no current before or behind the shower. Taking all together we have the situation of a moving charge, moving with almost the vacuum velocity of light, even though the electrons and positrons are moving slower. For a consistent picture one must not forget the positive ions, which are usually not considered when talking about the shower. They are very slow, but their position of creation moves with the velocity of light (shower front), as well as the position of the “charge neutralization” at the “shower tail”. The above picture is true with or without geo-magnetic field, in the former case the electrons and positrons move on curved trajectories due to the Lorentz force. Neglecting the finite dimension of the shower, one has a four-current

$$j(t', \vec{x}) = J(t') \delta^3(\vec{x} - \vec{\xi}(t')), \quad (1)$$

with a longitudinal component due to charge excess, and a transverse component due to the geo-magnetic field. The precise form of  $J(t')$  will be obtained from realistic shower simulations, using CONEX [14, 15]. Solving Maxwell's equations, we can express the electric field in terms of the four-current  $J$  and its

time derivative  $K = dJ/dt$ , evaluated at the retarded time.

In this paper, we will develop explicitly the formalism of electric fields created from general point-like currents of the form shown in eq. (1), in particular investigating carefully the role of a position dependent index of refraction. We analyze the electric fields for some typical high energy showers, their dependence on the observer position and on the orientation of the showers with respect to the magnetic field. We restrict ourselves to sufficiently large impact parameters, so that singularities (related to Cherenkov radiation) do not matter. In all cases, we can clearly relate the electric field signal to the sources. The dominant contribution comes always from the time variation of the currents. For finite angles between the shower axis and the magnetic field, the biggest contribution is due to the time derivative of the transverse currents induced by the geo-magnetic field; but there is also a contribution (three times smaller, opposite polarization) due to the transverse current itself. There is also a sizable contribution from the time derivative of the charge excess, and from the dipole moment. The strength of these two contributions is roughly 1/4 each compared to the dominant contribution from the transverse current. The fact that the time variation of the currents is the dominant mechanism leads to a characteristic bipolar signal.

These results actually confirm our earlier findings [13] of a bipolar signal due to the time derivatives of the sources. This is in qualitative contrast to the findings of [8, 9, 10, 11, 12], where a microscopic picture has been employed, leading to a single pulse. The fundamental difference is that the time variation of the currents in the macroscopic picture treats in an effective way the creation and disappearance of charges, which contributes significantly. In a microscopic picture this has to be treated explicitly.

## II. GEOMETRY

We characterize the trajectory of a moving point-like current (referred to as the shower trajectory) in the following way (see fig.1): we imagine a sphere around the center  $M_{\oplus}$  of the Earth with radius  $R_{\oplus} + a$ , with  $R_{\oplus}$  being the radius of the Earth. The point  $A$  is by definition the intersection of the trajectory with the sphere (supposed the intersection exists). The angle between the trajectory and the axis  $M_{\oplus}A$  (referred to as vertical) is called  $\theta$ . The trajectory is characterized by the point  $A$ , the angle  $\theta$  (and an azimuthal angle, which is not important for the following discussion). A position on the trajectory may be characterized by the distance  $d$

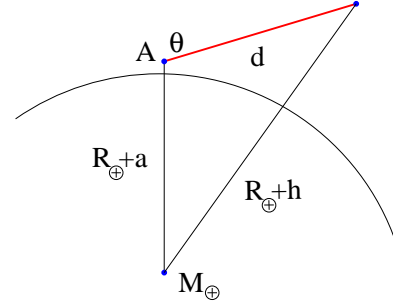


Figure 1: Characterizing the trajectory:  $A$  is the intersection of the trajectory with a sphere of radius  $R_{\oplus} + a$  around the center  $M_{\oplus}$  of the Earth, with  $R_{\oplus}$  being the radius of the Earth; the angle  $\theta$  measures the inclination.

from the point  $A$ . Using these definitions, the height along the trajectory is given as

$$h(d) = \sqrt{(R_{\oplus} + a)^2 + d^2 + 2(R_{\oplus} + a)d \cos \theta} - R_{\oplus}. \quad (2)$$

Let  $S$  be the point on the axis  $M_{\oplus}A$  representing the sea level. We define the “Earth frame”  $\{S, \vec{w}_x, \vec{w}_y, \vec{w}_z\}$  (see fig. 2) such that  $\vec{w}_z$  represents the vertical upward unit vector, and  $\vec{w}_y$  is orthogonal to the “shower plane” defined by the shower trajectory and the point  $S$ . In other words,  $\{S, \vec{w}_x, \vec{w}_z\}$  is the shower plane. The shower velocity vector is given as

$$\vec{V} = \begin{pmatrix} v \sin \theta \\ 0 \\ -v \cos \theta \end{pmatrix} \quad (3)$$

with respect to the Earth frame basis.

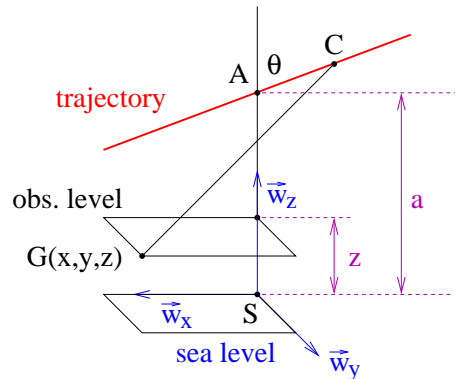


Figure 2: The trajectory as seen by an observer  $G$  situated on the observation level. We use the Earth frame  $\{S, \vec{w}_x, \vec{w}_y, \vec{w}_z\}$  to represent points and vectors.

In addition to the sea level plane we have to consider an “observation level plane” at some height  $z$

above sea level. We define an observation point  $G$  in the observation level plane with coordinates  $(x, y, z)$  with respect to the Earth frame. The point  $C$  represents the center of the air shower front at time  $t'$ , given as  $\vec{SC} = \vec{SA} + \vec{V}t'$ , with respect to the basis  $\vec{w}_i$ . The vector  $\vec{R} \equiv \vec{CG}$  is given as  $\vec{R} = \vec{SG} - \vec{SC}$ . We may define the point  $B$  of closest approach with respect to the observer. The distance from  $A$  is

$$d_B = x \sin \theta + (a - z) \cos \theta. \quad (4)$$

The impact parameter is

$$b = |\vec{BG}| = \sqrt{(x \cos \theta - (a - z) \sin \theta)^2 + y^2}. \quad (5)$$

We also define for later use

$$t_B = d_B/v \quad (6)$$

to be the time the shower passes at the position  $B$ .

Due to the magnetic field of the Earth, electrons and positrons move on spiral trajectories with opposite orientations, representing a transverse current [13]. This means, even when considering the shower as pointlike, the collective current  $\vec{J}$  is not simply a product of charge times velocity, there is in fact a component transverse to the shower velocity. We compute this current by using the CONEX shower simulation program, as

$$\vec{J} = \sum_{\text{positrons } i} e\vec{v}_i - \sum_{\text{electrons } j} e\vec{v}_j, \quad (7)$$

considering all electrons and positrons present at a given time. For calculating the currents, we employ

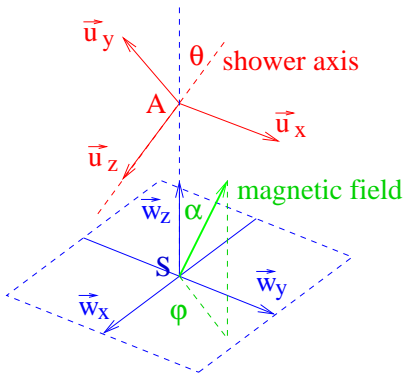


Figure 3: Reference frames.

the shower frame  $\{A, \vec{u}_x, \vec{u}_y, \vec{u}_z\}$ , see fig. 3, but the final results are expressed with respect to the Earth frame  $\{S, \vec{w}_x, \vec{w}_y, \vec{w}_z\}$ .

We will discuss the currents corresponding to air showers in more detail later, but it is useful already

at this point to have some idea about the times  $t'$  corresponding to shower maxima. The shower size and in particular the shower maximum depends primarily on the atmospheric depth, given as

$$X = X(t') = \int_{-vt'}^{\infty} \rho(h(x)) dx, \quad (8)$$

integrating along the trajectory. Here,  $h$  is the height above sea level, and  $\rho$  is the air density. The

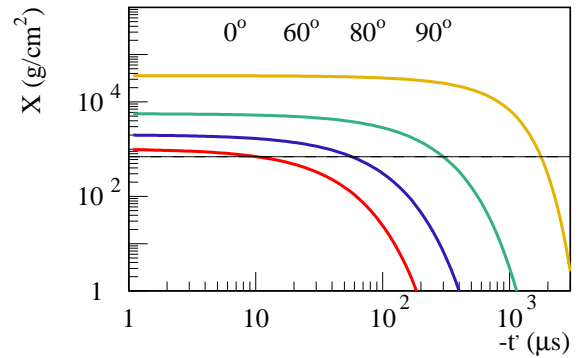


Figure 4: The depth versus the negative time  $-t'$ , for different angles (using always  $a = 140$  m). The horizontal line at  $X = 700$  g/cm<sup>3</sup> corresponds to the maximum of the charge distribution for showers with an energy of  $5 \cdot 10^{17}$  eV.

relation between  $X$  and  $t'$  (or  $d$ ) depends of course strongly on the angle  $\theta$ , as shown in fig. 4. Since we are interested in negative time  $t'$  (before the shower reaches  $A$ ), we plot  $X$  versus  $-t'$ . The horizontal line corresponds to the maximum of the charge distribution of showers with an energy of  $5 \cdot 10^{17}$  eV, which can be used to obtain the times  $t'$  corresponding to this maximum. Varying the angle  $\theta$  from  $0^\circ$  to  $90^\circ$ , the times range from some  $10 \mu\text{s}$  up to almost  $2000 \mu\text{s}$ . These numbers define the interesting time scales for the later discussions of retarded times.

### III. ELECTRIC FIELD DUE TO A GENERAL POINTLIKE SOURCE

Let us consider a point-like four-current,

$$j(t', \vec{x}) = J(t') \delta^3(\vec{x} - \vec{\xi}(t')), \quad (9)$$

for a given trajectory  $\vec{\xi}(t')$ , corresponding to the shower position  $C$  in the notation of the preceding

chapters. A moving charge corresponds to  $J^0 = qc$ ,  $\vec{J} = q\vec{v}$ , where  $c$  is the velocity of light. However, currents induced by the Earth's magnetic field require a more general treatment, which we are going to present in the following. In this chapter we investigate the case an index of refraction  $n$  equal to unity.

We first define the basic quantities of our approach. In order to obtain four-vectors  $x$  and  $\xi$ , we define  $x^0 = ct$  and  $\xi^0 = ct'$ . We will need the time derivative of the four-current  $J$  and of the four-vector  $\xi$ , and we define  $K = dJ/dx'^0$  and  $V = d\xi(t')/dx'^0$ . We consider here the case of a constant velocity  $V$ . Finally, we define  $R = (x - \xi(t'))$  to be the four-vector joining the position of the current  $\xi(t')$  and the position  $x$  of the observer.

The four-potential at point  $x$  is found to be

$$A = \frac{\mu_0}{4\pi} \frac{J}{|RV|}, \quad (10)$$

(see appendix), where all quantities are meant to be evaluated at the retarded time  $t^*$ . The three components of the electric field can be expressed as

$$E^i = c(\partial^i A^0 - \partial^0 A^i). \quad (11)$$

Taking also the  $x$  dependence of  $t^*$  into account, one gets (see appendix)

$$E^i = \frac{1}{4\pi\epsilon_0 c} \frac{L^{i0} - L^{0i}}{|RV|^3}, \quad (12)$$

with

$$L^{\alpha\beta} = RV R^\alpha K^\beta - RV J^\beta V^\alpha + VV R^\alpha J^\beta. \quad (13)$$

Concerning the denominator and possible singularities due to its roots, it is useful to note that

$$\frac{1}{|RV|} = \frac{|\partial t^*/\partial t|}{|\vec{R}|}, \quad (14)$$

from which one can see that possible singularities of the field coincide with singularities of the derivative  $\partial t^*/\partial t$ .

#### IV. REALISTIC INDEX OF REFRACTION

The index of refraction  $n$  in air varies spatially, mainly via its dependence on the altitude. We will study here the general case of an index of refraction being a function  $n(\vec{y})$  of the position  $\vec{y}$ . In this case we define curvilinear coordinates via the light curves passing through the position  $\vec{y}$ , see fig. 5. The optical path length,  $s$ , is defined as the travel time of a light signal multiplied by  $c$ . An elementary path

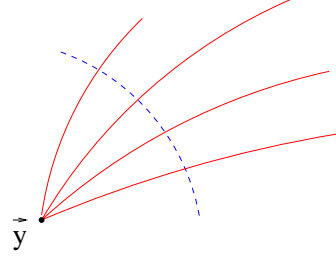


Figure 5: Light curves (full lines) in a medium with varying index of refraction. The dashed line represents a constant optical distance from the point  $\vec{y}$ .

length is expressed in terms of the components  $y^i$  of  $\vec{y}$  as  $ds^2 = n^2 dy^i dy^i$ . The equation for the derivatives  $v^k = dy^k/ds$  of the light curves is thus

$$\frac{dv^k}{ds} = -\Gamma_{ij}^k v^i v^j = \frac{n_k}{n} v^i v^i - 2 \frac{n_i}{n} v^k v^i, \quad (15)$$

where we used

$$\Gamma_{ij}^k = \frac{1}{n} (\delta_{ik} n_j + \delta_{kj} n_i - \delta_{ij} n_k), \quad (16)$$

with  $n_i = dn/dy^i$ . The light curves can be obtained by integrating this differential equation starting from some position  $\vec{y}_0$ . One gets a family of curves, characterized by the initial velocity vectors  $\vec{v}_0$  (more precisely by the two angles characterizing the direction of the initial velocity, since the module is given).

As the next step we discuss the effects of a varying index of refraction  $n(\vec{x})$  on the calculation of the electric field. The main difference compared to the case of  $n = 1$  is the fact that the condition for the retarded time, expressed via

$$\delta(R^0{}^2 - \vec{R}^2), \quad (17)$$

with  $R^0 = ct - ct'$  and  $\vec{R} = \vec{x} - \vec{\xi}$ , has to be modified by taking into account the curved light trajectories. We define a “distance”  $L = L(\vec{\xi}, \vec{x})$  to be the optical path length from the source position  $\vec{\xi}$  to the observer position  $\vec{x}$ , in other words  $L$  is the integral  $\int ds$  along the light curve from  $\vec{\xi}$  to  $\vec{x}$ . Instead of eq. (17), we now have

$$\delta(R^0{}^2 - L(\vec{\xi}(t'), \vec{x})^2), \quad (18)$$

which leads to

$$A = \frac{\mu_0}{4\pi} \frac{J}{|\vec{R}V|}, \quad (19)$$

with

$$\vec{R}^0 = c(t - t^*), \quad \vec{R}^i = -L \frac{\partial}{\partial \xi^i} L. \quad (20)$$

All quantities are meant to be evaluated at  $\vec{\xi}(t^*)$ , with the retarded time  $t^*$  corresponding to the roots of the argument of the  $\delta$  function in eq. (18). We thus get formally the same results as in the case  $n = 1$ , but with  $R$  replaced by  $\tilde{R}$ , and a different definition of  $t^*$ . The computation of the retarded times will be discussed in the next chapter.

Taking the derivative of  $R^{0^2} - L^2$ , we get the useful relation

$$\partial^\alpha ct^* = \frac{\bar{R}^\alpha}{\bar{R}V}, \quad (21)$$

with

$$\bar{R}^0 = c(t - t^*), \quad \bar{R}^i = L \frac{\partial}{\partial x^i} L, \quad (22)$$

which again relates possible singularities of the potential  $A$  (roots of the denominator) to singularities of  $dt^*/dt$ .

To compute the derivative  $\partial^\alpha A^\beta$  of the potential, we use

$$\partial^\alpha \tilde{R}V = \bar{V}^\alpha - \tilde{V}V \partial^\alpha ct^* \quad (23)$$

with the four-vectors  $\bar{V}$  and  $\tilde{V}$  given as

$$\bar{V}^\nu = \bar{g}^{\nu\mu} V_\mu, \quad \tilde{V}^\nu = \tilde{g}^{\nu\mu} V_\mu, \quad (24)$$

where the tensors  $\bar{g}$  and  $\tilde{g}$  are defined as

$$\bar{g}^{0\mu} = \bar{g}^{\mu 0} = \tilde{g}^{0\mu} = \tilde{g}^{\mu 0} = g^{\mu 0} \quad (25)$$

$$\bar{g}^{ij} = \frac{\partial}{\partial x^i} L \frac{\partial}{\partial \xi^j} L + L \frac{\partial}{\partial x^i} \frac{\partial}{\partial \xi^j} L, \quad (26)$$

$$\tilde{g}^{ij} = -\frac{\partial}{\partial \xi^i} L \frac{\partial}{\partial \xi^j} L - L \frac{\partial}{\partial \xi^i} \frac{\partial}{\partial \xi^j} L. \quad (27)$$

Making use of eq. (23) together with eq. (21), we finally can write the electric field as

$$E^i = \frac{1}{4\pi\epsilon_0 c} \frac{L^{i0} - L^{0i}}{|\tilde{R}V|^3}, \quad (28)$$

with

$$L^{\alpha\beta} = \tilde{R}V \bar{R}^\alpha K^\beta - \tilde{R}V \bar{V}^\alpha J^\beta + \tilde{V}V \bar{R}^\alpha J^\beta. \quad (29)$$

In case of  $n = 1$ , we have  $\tilde{R} = \bar{R} = R$ , as well as  $\tilde{g} = \bar{g} = g$ , and therefore  $\tilde{V} = \bar{V} = V$ , and we recover the formula derived earlier for the case  $n = 1$ .

It is of course not surprising to rediscover the  $n = 1$  case, but it is important to notice that the equation for the the field  $E^i$  in case of  $n > 1$  has the same structure as the one for  $n = 1$ , just with “ $\sim$ ” and “ $-$ ” decorated quantities instead of the “bare” ones. The former ones depend continuously

and smoothly on a parameter  $\delta$  which characterizes the deviation of  $n$  from unity. We have, for example,  $\tilde{R} = \bar{R}(\delta)$ , with  $\lim_{\delta \rightarrow 0} \tilde{R} = R$ , and thereafter  $\tilde{R} = R + R^{(1)}\delta + \dots$ . Since  $\delta < 0.0003$  we can actually already ignore to a good precision the linear term, in other words we can forget about all the “ $\sim$ ” and “ $-$ ” symbols, with two exceptions: first the term  $|\tilde{R}V|$  in the denominator can become very small, and here even a very small value of  $\delta$  could matter. Second the term  $\tilde{V}V$  is certainly very small ( $VV = 0$ ), but can be comparable to  $\tilde{R}V$ , close to a singularity. We finally obtain

$$E^i = \frac{1}{4\pi\epsilon_0 c} \frac{L^{i0} - L^{0i}}{|\tilde{R}V|^3}, \quad (30)$$

with

$$L^{\alpha\beta} = \tilde{R}V R^\alpha K^\beta - \tilde{R}V V^\alpha J^\beta + \tilde{V}V R^\alpha J^\beta. \quad (31)$$

In vector notation, we may write

$$\vec{E} = \vec{E}_{RK} + \vec{E}_{JV} + \vec{E}_{RJ}, \quad (32)$$

with

$$\vec{E}_{RK} = \frac{\vec{W}_{RK}}{D}, \quad \vec{E}_{JV} = \frac{\vec{W}_{JV}}{D}, \quad \vec{E}_{RJ} = \frac{\tilde{V}V}{\tilde{R}V} \frac{\vec{W}_{RJ}}{D}, \quad (33)$$

using  $D = 4\pi\epsilon_0 c (\tilde{R}V)^2$ , and with

$$\vec{W}_{AB} = \vec{A}B^0 - A^0\vec{B}. \quad (34)$$

Here, we assume  $\tilde{R}V > 0$ , to be verified later. The first two terms in eq. (33) are the contribution  $\vec{E}_{JV}$  due to the current  $J$ , and the contribution  $\vec{E}_{RK}$  due to the variation  $K = c^{-1} dJ/dt'$  of the current. The third contribution  $\vec{E}_{RJ}$  is small, unless one is close to a singularity, due to the smallness of the ratio  $\tilde{V}V/\tilde{R}V$ , for high energy showers with  $|\vec{V}| \approx 1$ .

As already mentioned (eq. (21)),  $|\tilde{R}V|$  may be expressed in terms of the derivatives of the retarded time, as  $|\tilde{R}V| = c(t - t^*)/(dt^*/dt)$ . We therefore should be very careful about the evaluation of the retarded time  $t^*(t)$  for a given observer time  $t$ , where the precise values of  $n$  may be important even though  $n - 1$  is very small.

## V. RETARDED TIME

The retarded time is obtained from solving  $L = R^0$ , which may be written as

$$L(\vec{\xi}(t'), \vec{x}) - c(t_B - t') = c(t - t_B), \quad (35)$$

where a term  $-ct_B$  has been added on both sides, for later convenience. The time  $t_B$  corresponds to

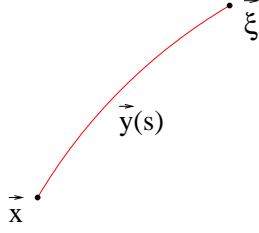


Figure 6: Light curve joining  $\vec{x}$  and  $\vec{\xi}$ .

the time when the shower is closest to the observer position  $\vec{x}$ .

We first evaluate the l.h.s. of eq. (35), for a given arbitrary value of  $t'$ , corresponding to some shower position  $\vec{\xi}(t')$ . To obtain  $L$ , we solve the differential equation

$$\frac{dy^k}{ds} = v^k, \quad \frac{dv^k}{ds} = \frac{n_k}{n} v^i v^i - 2 \frac{n_i}{n} v^k v^i, \quad (36)$$

with the boundary conditions

$$\vec{y}(0) = \vec{x}, \quad \vec{y}(s^*) = \vec{\xi}, \quad (37)$$

with  $s^*$  to be determined (see fig. 6). The index of refraction  $n$  is

$$n(\vec{y}) = 1 + 0.226 \frac{\text{cm}^3}{g} \rho(h(\vec{y})), \quad (38)$$

with  $\rho$  being the density of air and  $h(\vec{y})$  the atmospheric height  $h$  corresponding to a position  $\vec{y}$ . We employ an adaptive step-size Bulirsch-Stoer algorithm to integrate very efficiently the differential equation, and the three-dimensional Newton-Raphson formula to accommodate the boundary conditions. Having solved this problem means having found an  $s^*$  which corresponds to the optical path length joining  $\vec{\xi}$  and  $\vec{x}$ , so

$$L(\vec{\xi}(t'), \vec{x}) = s^*. \quad (39)$$

To understand the results, it is useful to consider two limiting cases, namely  $n = 1$  and  $n = n_{\text{ground}} \approx 1.0003$  (the reality lying in between). For constant  $n$ , the l.h.s. of eq. (35) reads

$$L - c(t_B - t') = n|\vec{R}| - c(t_B - t'), \quad (40)$$

where  $\vec{R}$  has been defined earlier to be the vector joining the emission point on the shower and the position of the observer. One gets

$$L - c(t_B - t') = n\sqrt{v^2(t_B - t')^2 + b^2} - c(t_B - t'). \quad (41)$$

The expression  $L - c(t_B - t')$  divided by  $b$  is an universal function of  $\tau = c(t_B - t')/b$ , namely

$$n\sqrt{\beta^2\tau^2 + 1} - \tau, \quad (42)$$

with  $\beta = v/c$ . For  $n = 1$  and  $\beta < 1$ , we have a monotonically decreasing function with no lower limit. In all the following considerations, we always consider a fast shower, with  $v = c$ , so  $\beta = 1$ . In this case, we still have a monotonically decreasing function, but with a lower limit equal to zero (for  $\tau \rightarrow \infty$ ). Keeping  $\beta = 1$ , but taking  $n > 1$ , the curve reaches a minimum at some finite value of  $\tau$ , and then increases. We show the corresponding results in fig. 7, where we plot  $L - c(t_B - t')$  versus  $t_B - t'$ , for two impact parameters  $b$  and several inclinations. The dashed curve refers to  $n = 1$ , the dotted one to  $n > 1$ . To underline the scaling behavior, we scaled abscissas and ordinates as  $1/b$ , and indeed we observe, for all angles and impact parameters, the same curves, for the two limiting cases with constant  $n$ .

Also shown in fig. 7 are the curves  $L - c(t_B - t')$  versus  $t_B - t'$ , for the case of a realistic index of refraction (full lines), obtained from the numerical procedures discussed above. As expected, these curves are well in between the two limiting cases  $n = 1$  and  $n = n_{\text{ground}}$ . The scaling is violated: depending on impact parameter and inclination, the exact curve follows more closely either the  $n = 1$  or the  $n = n_{\text{ground}}$  case. Whereas for vertical showers the exact curves are close to the  $n = 1$  case, we see an increasing deviation with increasing inclination, up to the extreme at  $90^\circ$ , where the curves are close to the results for  $n = n_{\text{ground}}$ . All this is understandable, since, with increasing angle, even light emitted at early times (large  $t_B - t'$ ) travels more and more at  $n \approx n_{\text{ground}}$ . It should be noted that at very large  $t_B - t'$ , the curves  $L - c(t_B - t')$  approach a constant, for obvious reasons, and there will be a (at least one) turning point.

The retarded time  $t' = t^*$  is the solution of

$$L - c(t_B - t') = c(t - t_B), \quad (43)$$

for a given observer time  $t$ . In other words,  $t^*$  is the intersection of the curves  $L - c(t_B - t')$ , shown in fig. 7, with a horizontal line with ordinate  $c(t - t_B)$ . In the range of  $t_B - t'$  up to  $3000 \mu\text{s}$  (useless to go to earlier times), we have no solution for  $t < t_{\text{min}}$ , while for larger values there are one, two, or even more solutions. For the minimum time we have  $t_{\text{min}} > t_B$ , where the precise value depends on angle and impact parameter. We compute the retarded times  $t^*$  numerically. A first estimate is obtained via interpolation using tables of  $L - c(t_B - t')$ , a refinement is obtained by again solving the differential equation eq. (36), but now with the boundary condition

$$\vec{y}(0) = \vec{x}, \quad \vec{y}(t - t^*) = \vec{\xi}. \quad (44)$$

Only few Newton-Raphson iterations are needed to get a very high precision. The results are shown in

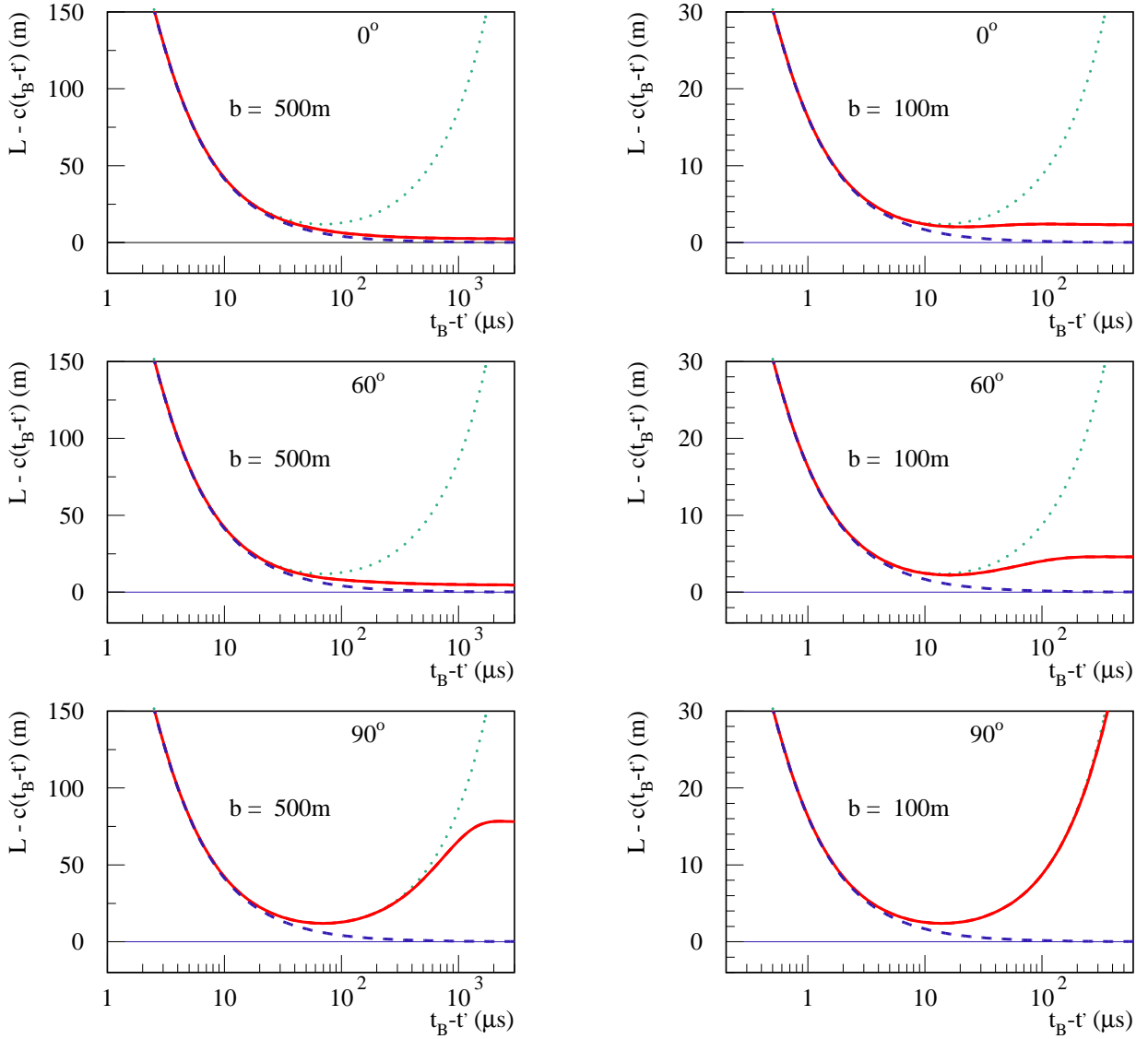


Figure 7: The optical path length  $L(\vec{\xi}(t'), \vec{x})$  minus  $c(t_B - t')$  versus  $t_B - t'$ , for impact parameters of 500 m and 100 m, for different angles. The solid lines represent the results for a realistic variable index of refraction. The other curves refer to calculations for a constant  $n$ : namely  $n = 1$  (dashed) and  $n = n_{\text{ground}} \approx 1.0003$  (dotted).

fig. 8, where we plot  $t_B - t^*$  versus  $t - t_B$ , with  $t^*$  being the retarded time. We get of course what we expect after the above discussion. In case of  $n = 1$ , we have no solution for negative  $t - t_B$ , for positive values there is exactly one solution, representing a monotonically decreasing curve. The other limiting case  $n = n_{\text{ground}}$  provides a two-valued curve and we have two solutions for  $t - t_B$  being bigger than some minimum value, no solutions otherwise. The results for a realistic index of refraction (full lines) lies in between the two limits. For large impact parameters (like 500 m), the exact curves are close to the  $n = 1$  case, with increasing angle and decreasing impact

parameter, the curves get more and more close to the other limiting case, leading to two or even more retarded times, for a given observer time  $t$ . This means that for the electric fields one has to sum up the contributions due to several retarded times, if the currents  $J(t^*)$  at these times are non-zero.

From the above discussion – and in particular from the comparison of the exact calculation with the limiting cases of constant index of refraction – one gets the impression that the main effect is not really due to curved light trajectories but to the fact that the index changes along the trajectory. In order to verify the conjecture, we compute the optical path length

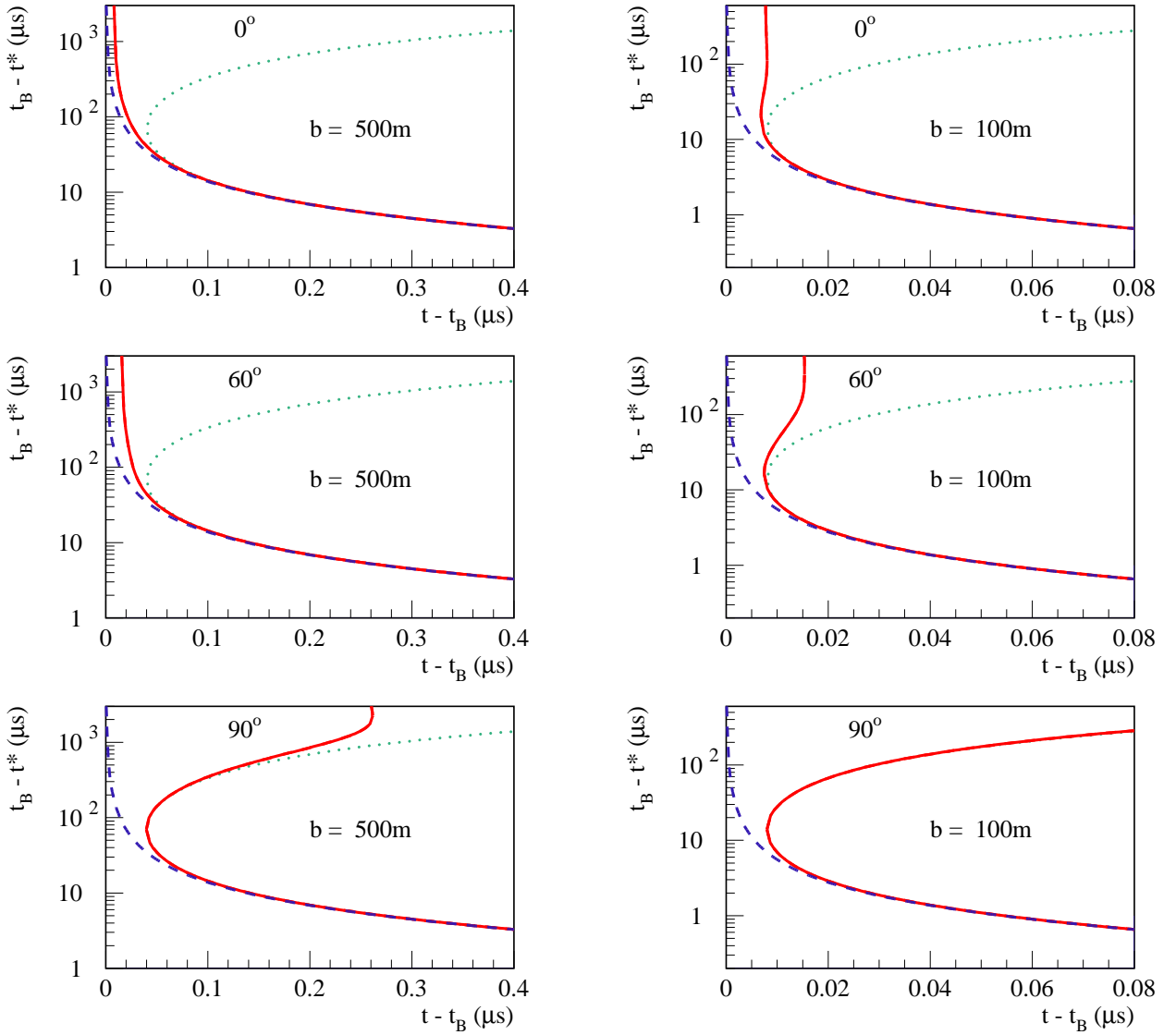


Figure 8: The retarded time expressed via  $t_B - t^*$  versus observer time  $t - t_B$ , for impact parameters of 500 m and 100 m, for different angles. The solid lines represent the results for a realistic variable index of refraction. The other curves refer to calculations for a constant  $n$ : namely  $n = 1$  (dashed) and  $n = n_{\text{ground}} \approx 1.0003$  (dotted).

in “straight line approximation” as

$$L_{\text{straight}}(\vec{\xi}(t'), \vec{x}) = \int_{GC} n(\vec{y}) ds, \quad (45)$$

where  $GC$  is the straight line joining observer position  $\vec{x}$  and charge  $\vec{\xi}(t')$ . Subsequently we compute the retarded times by solving  $L_{\text{straight}} = R^0$ . The results are shown in fig. 9 as dotted lines, together with the exact curves (full lines). The two results are almost indistinguishable, with the only exception of a small deviation for  $b = 500\text{m}$  and  $\theta = 90^\circ$ , at very early retarded times. The straight line approximation is therefore for most applications largely suffi-

cient.

A delicate point is related to the derivative  $\partial t^*/\partial t$ . We have

$$\frac{1}{\widetilde{RV}} = \frac{1}{c(t - t^*)} \frac{\partial t^*}{\partial t}, \quad (46)$$

showing that possible singularities of the expression for the electric field, corresponding to the roots of  $\widetilde{RV}$ , are related to singularities of  $\partial t^*/\partial t$ . In the simplest case of a large impact parameter and small angles,  $t_B - t^*$  is a monotonic function of  $t - t_B$ , and thus  $\partial t^*/\partial t$  is as well, as shown in fig. 10. Compared to the case  $n = 1$  (dashed) the exact



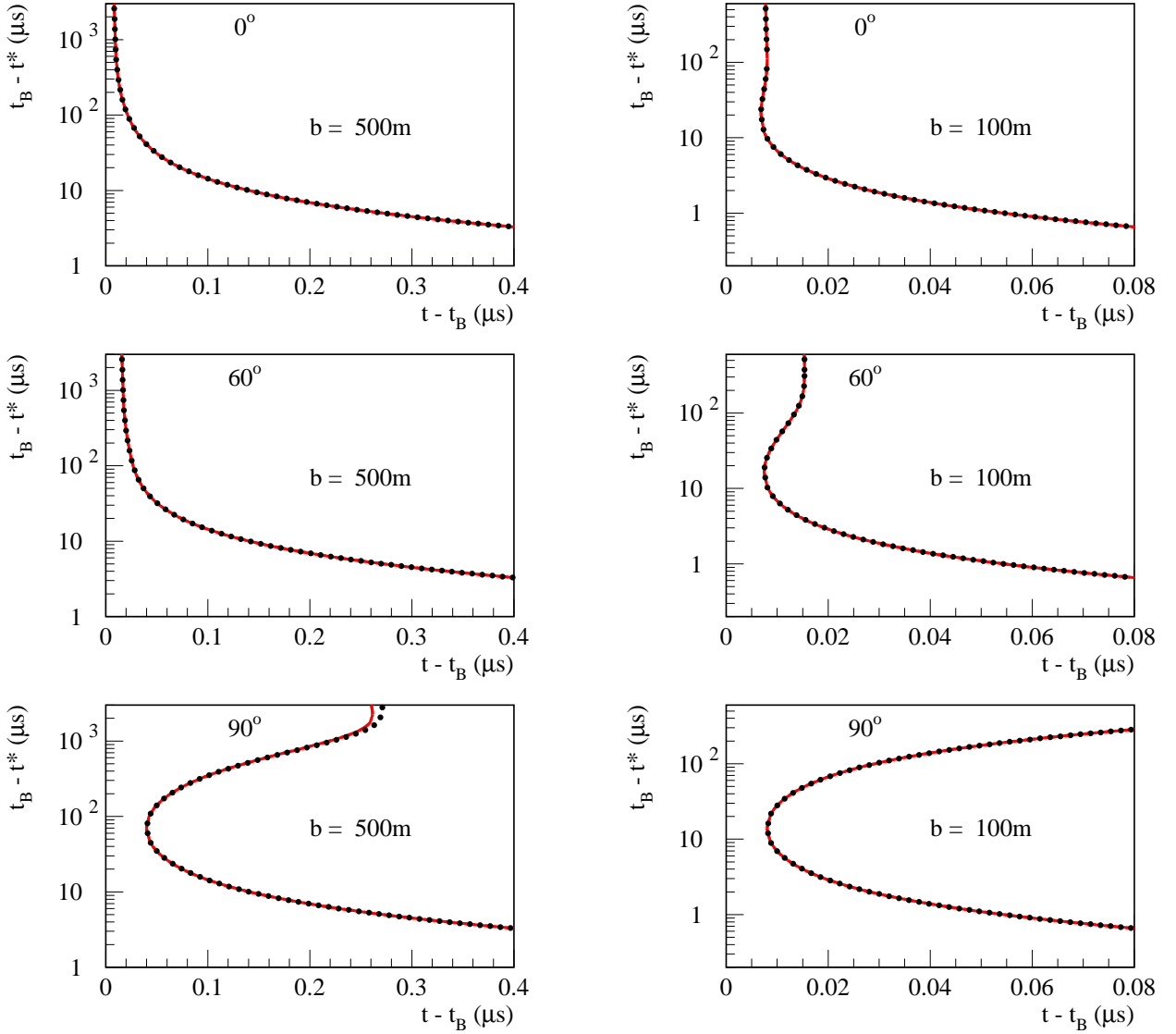


Figure 9: The retarded time expressed via  $t_B - t^*$  versus observer time  $t - t_B$ , for impact parameters of 500 m and 100 m, for different angles, considering a realistic variable index of refraction. The solid lines represent the exact results, the dotted lines refer to the “straight line approximation”.

curve (full line) grows more rapidly for  $t - t_B \rightarrow 0$ . For larger angles, we obtain singular points, where  $\partial t^*/\partial t$  diverges. This means that whenever we have a situation where  $dt^*/dt$  is singular, and in addition the current is non-vanishing at the corresponding retarded time, we have to consider the finite extension of the source, which amounts to an integration over the (square root) singularity, which gives a finite result.

It should be noted that the singularities of  $\partial t^*/\partial t$  correspond to the singularities that gives rise to Cherenkov radiation. It reflects the fact that electromagnetic waves emitted at different times arrive

simultaneously at the observer position.

The retarded time where the first singularity may occur depends on the impact parameter: it is proportional to  $b$ . It is somewhat larger than  $10 \mu\text{s}$  for  $b = 100 \text{ m}$ , corresponding to a source more than 3 km away.

To avoid this discussion related to singularities for the moment (to be treated in a forthcoming publication), we restrict ourselves to situations which are “well behaved” in the sense that  $\partial t^*/\partial t$  is nonsingular there where the currents are non-vanishing.

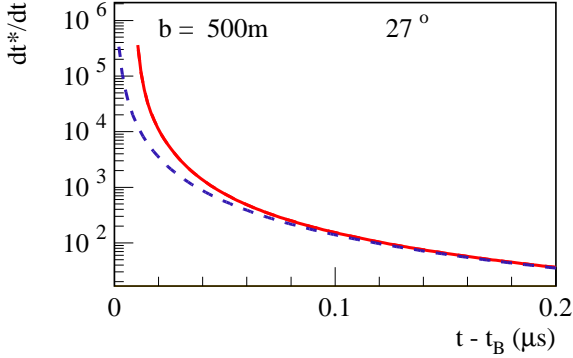


Figure 10: The derivative  $dt^*/dt$  versus  $t - t_B$ , for  $b = 500$  m and  $\theta = 27^\circ$ , in case of a realistic index of refraction (full line) and the case  $n = 1$  (dashed).

## VI. THE ROLE OF THE POSITIVE IONS

For the individual charged particles the magnitude of  $J^0$  turns out to be always bigger than that of  $J^z$ , even if one turns off the magnetic field. This is due to the fact that the electrons move slower than the shower front. They are constantly losing energy and eventually drop out. Close to the shower maximum we have a steady state since here the number of net charge created is equal to the net charge dropped. On the other hand, the net charge created must correspond to a corresponding positive charge in terms of ionized atoms, and therefore the net charge behind the shower (and in front of it anyway) is zero. So we have effectively a moving charge, moving with the speed of the shower front, which means that the  $z$  and the  $0$  component of the total, collective, effective current must be equal. As mentioned above, we do not get this identity if we would only consider electrons and positrons, and not the ions. The ions will contribute to  $J^0$ , not to the other components of the current (they are not moving) to yield finally  $J_{\text{tot}}^0 = J_{\text{tot}}^z \equiv J^z$ , where “tot” refers to the fact that we consider all, electrons and ions. In the following calculations, we will always use  $J_{\text{tot}}^0 = J^z$ , although strictly speaking this is only valid close to the maximum, but on the other hand the most important contribution to the fields is due to the charges close to the maximum. For the rest of the paper  $J$  will refer to the total current, including the ion part.

The property  $J^0 = J^z$  has important consequences concerning the polarity of the signal. The

electric field is given as a sum of three terms,

$$\vec{E}_{JV} = \frac{\vec{W}_{JV}}{D}, \quad \vec{E}_{RK} = \frac{\vec{W}_{RK}}{D}, \quad \vec{E}_{RJ} = \frac{\tilde{V}V}{\tilde{R}V} \frac{\vec{W}_{RJ}}{D}, \quad (47)$$

with  $\vec{W}_{AB} = \vec{A}B^0 - A^0\vec{B}$ . We may split the vectors  $\vec{W}$  into components parallel and orthogonal to the shower axis. The components of the shower velocity are  $V^0 = 1$ ,  $\vec{V}^\perp = 0$ ,  $V^\parallel = \beta$ , with  $\beta$  being very close to unity. We thus find

$$W_{JV}^\parallel = J^0(1 - \beta) \approx 0 \quad (48)$$

and

$$\vec{W}_{JV}^\perp = \vec{J}^\perp. \quad (49)$$

So the field  $\vec{E}_{JV}$  is almost purely transverse, parallel to the transverse current, as sketched in figs. 11, where we show the electric field vectors for four different observers situated in a plane transverse to the shower axis.

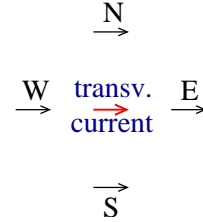


Figure 11: The electric field vectors from the contribution  $\vec{E}_{JV}$ , being proportional to the transverse current  $\vec{J}^\perp$ .

Furthermore, we find  $W_{RK}^\parallel \approx \tilde{R}V K^0$ , (where “ $\approx$ ” here means correct to a precision of  $n - 1$ ) which can be proven by using  $1 = (\partial^0 - \partial^\parallel)ct^* \approx (R^0 - R^\parallel)/\tilde{R}V$ , due to time translation invariance. Since the field in general is large when  $\tilde{R}V$  is small, we may conclude that  $\vec{W}_{RK}^\parallel$  is small compared to the transverse component, which we express as

$$W_{RK}^\parallel = \tilde{R}V K^0 \approx 0. \quad (50)$$

For the transverse part we find

$$\vec{W}_{RK}^\perp = \vec{R}^\perp K^0 - R^0 \vec{K}^\perp, \quad (51)$$

which means that here not only the transverse current (or better: its time derivative) contributes, but also the longitudinal one via  $K^0$ . Whereas the latter one is radial with respect to the axis, the former one is anti-parallel to the direction of the transverse current, see fig. 12.

We said earlier that the third term  $\vec{E}_{RJ}$  is small, away from singularities; let us investigate this term

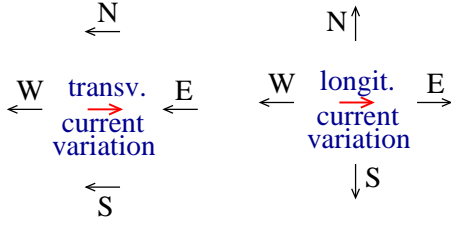


Figure 12: The electric field vectors from the contribution  $\vec{E}_{RK}$ ; one part is proportional to the time variation  $\vec{K}^\perp$  of the transverse current  $\vec{J}^\perp$  (left plot), a second part is proportional to the variation  $K^0$  of the longitudinal current, and proportional to  $\vec{R}^\perp$  and therefore radial (right plot).

more closely. Using the same arguments as for  $W_{RK}$ , we find

$$E_{RJ}^\parallel = \frac{\tilde{V}V}{\tilde{R}V} \frac{\tilde{R}V J^0}{D} = \tilde{V}V \frac{J^0}{D} \approx 0, \quad (52)$$

where “ $\approx 0$ ” means small compared to the transverse component, which is

$$\vec{E}_{RJ}^\perp = \frac{\tilde{V}V}{\tilde{R}V} \frac{\vec{R}^\perp J^0 - R^0 \vec{J}^\perp}{D}. \quad (53)$$

Lets us consider (just here, for an estimate) a constant index of refraction  $n > 1$  and let us assume that  $\beta > n^{-1}$ . The prefactor  $\tilde{V}V/\tilde{R}V$  would then be proportional to  $\gamma^{-2}(1 - n\beta \cos\alpha)^{-1}$ , with  $\alpha$  being the angle between the shower axis and  $\vec{R}$ . Even though  $\gamma$  is large, the term contributes when  $n\beta \cos\alpha$  approaches unity, which corresponds to the above-mentioned singularity. This is actually the well known “Cherenkov radiation”. It should be noted that these singularities have to be treated very carefully, using the realistic position dependent index of fraction  $n(\vec{y})$ , and naively replacing  $\tilde{V} \vec{R}$  by  $V$  and  $R$  is certainly not permitted. In this paper we restrict ourselves to not too small impact parameters, where the contribution  $\vec{E}_{RJ}$  is negligible.

## VII. DIPOLE FIELD

So far we discussed electric fields created by the current due to the charge excess – taking into account the positive ions – and the fields due to transverse current induced by the geomagnetic field. However, this magnetic field does not only create a transverse current, but also a dipole moment  $\vec{P}$  originating from the separation of the electric charges [5, 13]. We define  $q$  to be the product  $Ne$  of the number of electrons and positrons multiplied by the

elementary charge  $e$ , and we define the derivatives of  $q$  as  $q_n = c^{-n} \partial^n q / dt^n$ , for  $n = 1, 2$ . The ratios  $M^k = P^k/q$  are slowly varying (compared to the variation of  $q$ ) along the trajectory. The potential due to this dipole moment may be written as

$$A_{\text{dip}}^\beta = -\vec{M} \vec{\nabla} A_q^\beta = -M^k \partial_k A_q^\beta, \quad (54)$$

where  $A_q^\beta$  is the potential due to the current  $J_q = cqV$ , representing a moving charge  $q$ . The electric dipole field is then given as

$$E_{\text{dip}}^i = -M^k \partial_k E_q^i, \quad (55)$$

with  $E_q^i$  being the electric field due to a moving charge  $q$ . We may use the formulas derived earlier, where the electric field is given as a sum of three contributions. Only one term ( $\vec{E}_{RK}$ ) is dominant, if we are not close to a singularity, with  $K = cq_1V$ . The dipole field can then be written as

$$E_{\text{dip}}^i = -\frac{1}{4\pi\epsilon_0} M^k \partial_k q_1 \frac{R^i V^0 - R^0 V^i}{(\tilde{R}V)^2} \quad (56)$$

$$= -\frac{1}{4\pi\epsilon_0} M^k \left\{ q_2 (\partial_k ct^*) \frac{R^i V^0 - R^0 V^i}{(\tilde{R}V)^2} + q_1 \partial_k \frac{R^i V^0 - R^0 V^i}{(\tilde{R}V)^2} \right\}. \quad (57)$$

The identities

$$\partial_k R^\alpha = g_k^\alpha - V^\alpha \partial_k ct^*, \quad (59)$$

$$\partial_k \tilde{R}V = \tilde{V}_k - \tilde{V}V \partial_k ct^*, \quad (60)$$

$$\partial_k ct^* = \tilde{R}_k / \tilde{R}V, \quad (61)$$

allow us to obtain

$$\vec{E}_{\text{dip}} = -q_1 \frac{\vec{M}}{D_2} + q_2 \frac{(\vec{M}\vec{R}) \vec{W}_{RV}}{D_3} + q_1 \frac{2\tilde{V}V (\vec{M}\vec{R}) \vec{W}_{RV}}{D_4}, \quad (62)$$

with the denominators given as

$$D_n = 4\pi\epsilon_0 (\tilde{R}V)^n, \quad (63)$$

and with  $\vec{W}_{AB} = \vec{A}B^0 - A^0\vec{B}$ . The last term in eq. (62) only contributes close to a singularity, and for all the applications in the following chapters we only consider the first two terms.

We may again split the vectors into longitudinal and transverse parts, with respect to the shower axis. Let us consider the dominant second term. We have  $\vec{W}_{RV} \approx 0$ , following the same arguments which lead to the conclusion that  $\vec{W}_{RK}$  is small. Therefore also the dipole field is essentially transverse. Using

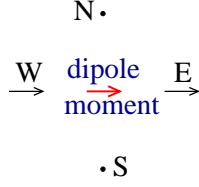


Figure 13: The electric field vectors from the dominant dipole contribution, being proportional to the projection of  $\vec{M}$  to the radial vector pointing to the observer.

$\vec{W}_{RV}^\perp = \vec{R}^\perp$  and the fact that  $\vec{M}$  is purely transverse, we get

$$\vec{E}_{\text{dip}} \approx q_2 \frac{(\vec{M} \vec{R}^\perp)}{D_3} \vec{R}^\perp = q_2 \frac{(\vec{M} \vec{R}^\perp)}{D_3} \vec{R}^\perp, \quad (64)$$

which means that the field is proportional to the projection of  $\vec{M}$  to the radial vector pointing to the observer, as shown in fig. 13.

### VIII. SHOWER PARALLEL TO THE MAGNETIC FIELD

In the following, we consider the case of a shower with an initial energy of  $5 \cdot 10^{17}$  eV, an inclination  $\theta = 27^\circ$ , and an azimuth angle  $\psi = 180^\circ$ , defined with respect to the magnetic north pole, see fig. 14. The angle  $\psi$  refers to the origin of the shower, it is related to the angle  $\varphi$  from the preceding chapter as  $\psi = 180^\circ - \varphi$ . So  $\psi = 180^\circ$  thus implies that the shower moves from south to north. We consider the magnetic field at the CODALEMA site, i.e.  $|\vec{B}| = 47.3 \mu\text{T}$  and  $\alpha = 153^\circ$ , so the shower moves parallel to the magnetic field. We consider an observer at  $x = 0$ ,  $y = 500$  m,  $z = 140$  m. We suppose  $a = z$  (so the shower hits the ground at  $x = y = 0$ ). The coordinates  $x$ ,  $y$ ,  $z$  are defined in the Earth system.

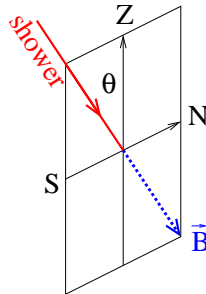


Figure 14: South-north shower ( $\theta = 27^\circ$ ,  $\psi = 180^\circ$ ), being parallel to the geo-magnetic field.

The electron number  $N$  reaches its maximum at about  $-15 \mu\text{s}$ , reaching almost  $4 \cdot 10^8$  particles, as

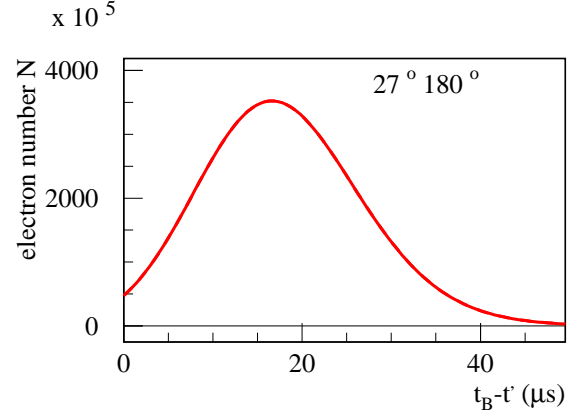


Figure 15: The number  $N$  of electrons and positrons, as a function of the time  $t_B - t'$ .

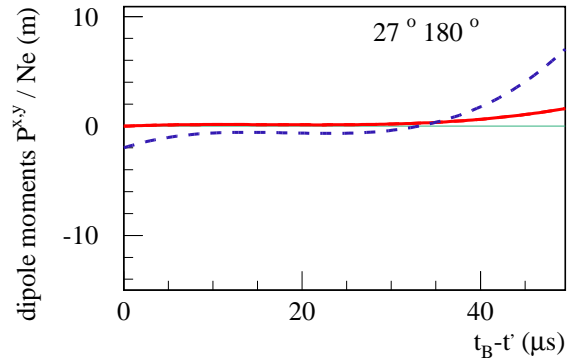
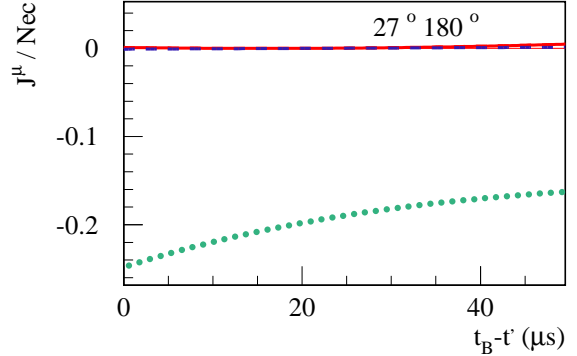


Figure 16: The  $x$ - (full line),  $y$ - (dashed) and  $z$ -component (dotted) of the current  $J$  divided by  $Nec$  (upper plot), and the  $x$ - (full line), and  $y$ -component (dashed) of the dipole moment  $P$  divided by  $Ne$ , (lower plot), as a function of the retarded time. The vector components refer to the shower frame.

shown in fig. 15. It is useful to plot the components of the current, divided by  $Nec$ , with

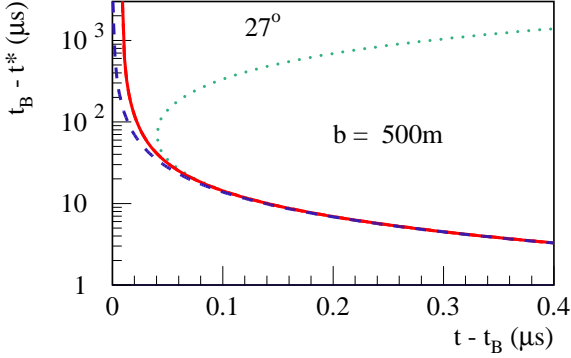


Figure 17: The retarded time expressed via  $t_B - t^*$  versus observer time  $t - t_B$ , for  $b = 500$  m and  $\theta = 27^\circ$ . The solid lines represent the results for a realistic variable index of refraction, the two other curves to  $n = 1$  and  $n = n_{\text{ground}}$ .

$e$  being the electron charge, and  $c$  the velocity of light, see fig. 16. The components  $J^x/Nec$  and  $J^y/Nec$  represent the average transverse drift velocity, in units of  $c$ , caused by the magnetic field. For the present example, the components  $J^x/Nec$  and  $J^y/Nec$  are zero. This is understandable, since the average transverse drift velocity is zero for showers moving parallel to the magnetic field. The component  $J^z/Nec$  represents the charge excess which stays almost constant at a value around -0.2. The time variation of the currents is mainly due to the time variation of  $N$ . For the numerical calculations, also the small time variations of  $J^z/Nec$  are taken into account. In fig. 16, we also plot the components  $P^x$  and  $P^y$  of the dipole moment divided by  $Ne$ . As expected, the dipole moment is close to zero. It is not exactly zero due to statistical fluctuations in regions where  $Ne$  is small. The actual Monte Carlo results are strongly fluctuating around zero, the curves shown in fig. 16 is obtained after smoothening the “raw data”.

In the expressions for the electric fields at some observer time  $t$ , the currents  $J$  and their derivatives  $K$  appear, evaluated at the retarded time  $t^*$ . Following the procedure discussed earlier, we compute  $t^*(t)$ , as shown in fig. 17. We see that a shower maximum at  $t_B - t^* \approx 15 \mu\text{s}$  corresponds to  $t - t_B \approx 0.1 \mu\text{s}$ . Given the time dependence  $J(t')$  of the current and the relation  $t^*(t)$  between the retarded time and the observation time  $t$ , we may present the current as  $J(t^*(t))$  versus the observer time. In fig. 18, we show the components of the current and their derivatives in the Earth frame. The  $y$ -component vanishes, as expected, since this is the component perpendicular to the shower plane (containing the shower axis and

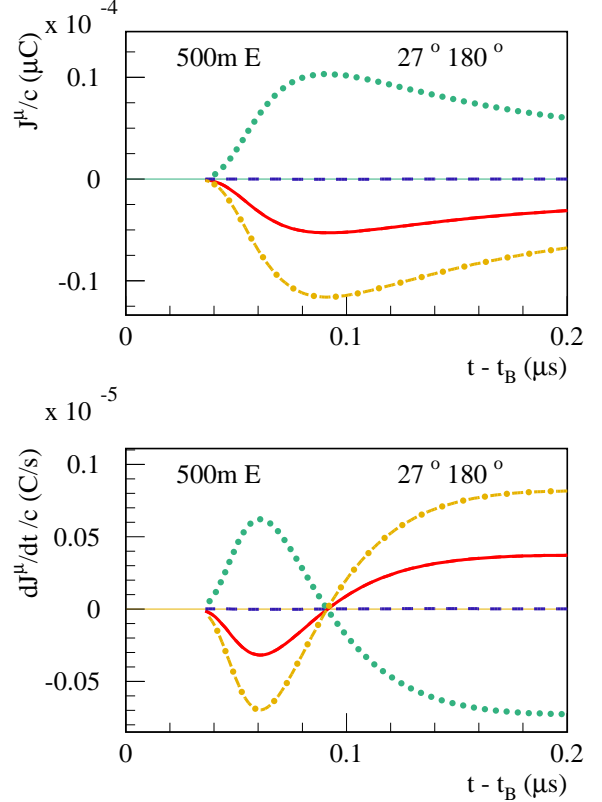


Figure 18: The  $x$ - (full line),  $y$ - (dashed),  $z$ - (dotted), and 0-component (dashed-dotted) of the current  $J$  and their derivatives (bottom) versus the observer time  $t$ . Here we consider the total current, including the ion contribution. The vector components refer to the Earth frame.

the vertical axis). One should note that the width of  $J(t')$  is of the order of  $10 \mu\text{s}$ , whereas the width of  $J$  versus observer time is just a fraction of a micro second.

We are now ready to discuss the electric fields. As shown earlier, we have

$$\vec{E} = \vec{E}_{\text{dip}} + \vec{E}_{RK} + \vec{E}_{JV}, \quad (65)$$

with the dipole field  $\vec{E}_{\text{dip}}$  and with

$$\vec{E}_{RK} = \frac{\vec{W}_{RK}}{D}, \quad \vec{E}_{JV} = \frac{\vec{W}_{JV}}{D}, \quad (66)$$

using

$$D = 4\pi\epsilon_0 n^2 (\tilde{R}V)^2$$

and

$$\vec{W}_{AB} = \vec{A}B^0 - A^0\vec{B}, \quad (67)$$

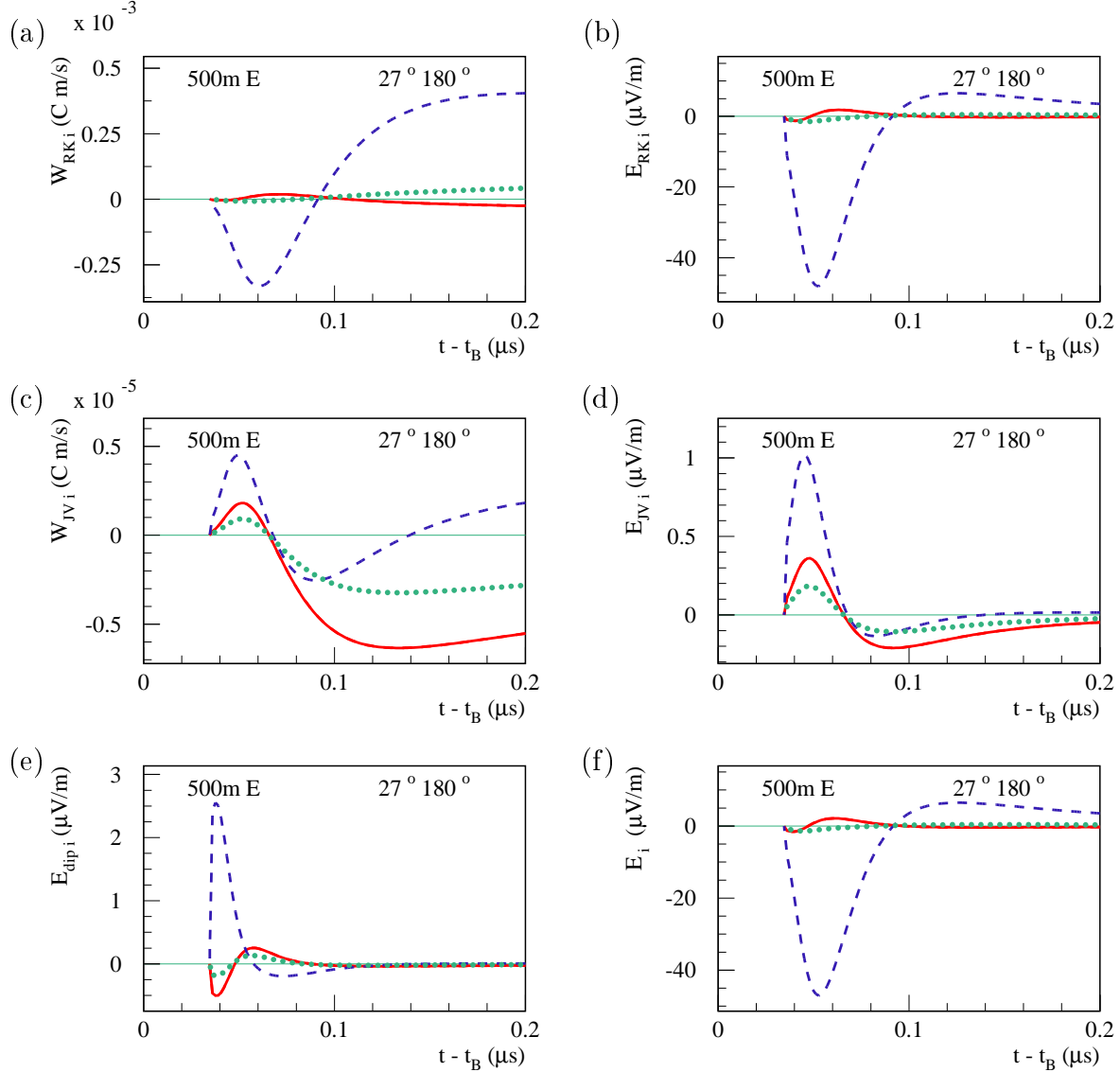


Figure 19: The  $x$ - (full line),  $y$ - (dashed) and  $z$ -component (dotted) of  $\vec{W}_{RK}$  (a),  $\vec{W}_{JV}$  (c), and of the corresponding fields  $\vec{E}_{RK}$  (b),  $\vec{E}_{JV}$ (d), the dipole contribution  $\vec{E}_{dip}$  (e), and the components of the total electric field, with all contributions (f). The vector components refer to the Earth frame.

for two four-vectors  $A$  and  $B$ . The three components of the vectors  $\vec{W}$  and the corresponding field contributions, as well as the three components of the complete field  $\vec{E}$  are shown in fig. 19. The dipole field is of course negligible. The contribution  $\vec{E}_{RK}$  – having its origin in the time variation  $K$  of the currents – is by far dominant. Only the  $y$ -component is sizable, meaning that the field is oriented radially compared to the shower axis (the observer sits on the  $y$ -axis). The contribution  $\vec{E}_{JV}$  is very small, in comparison. This can easily be understood since here, without transverse drift, we have essentially a longitudinally moving charge, and in such a case  $\vec{J}\vec{V}^0 - J^0\vec{V}$  vanishes.

## IX. SHOWER WITH A LARGE ANGLE WITH RESPECT TO THE MAGNETIC FIELD

In the following, we consider a shower with an initial energy of  $5 \cdot 10^{17}$  eV, an inclination  $\theta = 27^\circ$ , and an azimuth angle  $\psi = 0^\circ$ , defined with respect to the magnetic north pole, see fig. 20.

The angle  $\psi$  refers to the origin of the shower, it is related to the angle  $\varphi$  from the preceding chapter as  $\psi = 180^\circ - \varphi$ . So  $\psi = 0$  means the shower moves from north to south. We consider again the magnetic field at the CODALEMA site, so the shower makes an angle of roughly  $54^\circ$  with the magnetic

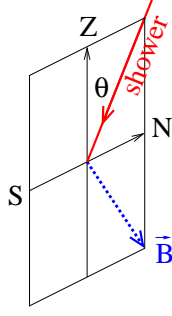


Figure 20: North-south shower ( $\theta = 27^\circ$ ,  $\psi = 0^\circ$ ).

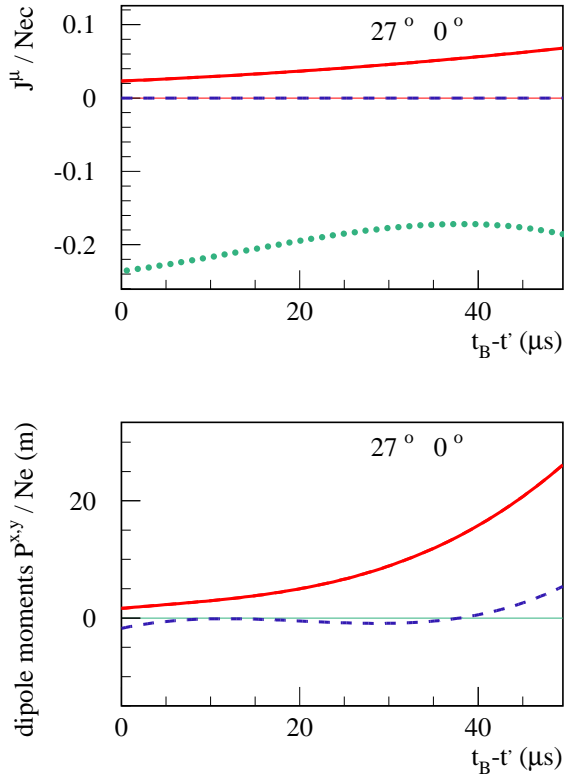


Figure 21: The  $x$ - (full line),  $y$ - (dashed) and  $z$ -component (dotted) of of the current  $J$  divided by  $Nec$  (upper plot), and the  $x$ - (full line), and  $y$ -component (dashed) of of the dipole moment  $P$  divided by  $Ne$  (lower plot), as a function of of the time  $t_B - t'$ . The vector components refer to the shower frame.

field. We consider an observer at  $x = 0$ ,  $y = 500$  m,  $z = 140$  m (which means: east of the impact point). We suppose  $a = z$  (so the shower hits the ground at  $x = y = 0$ ). We plot again the components of the current, divided by  $Nec$ , with  $e$  being the electron charge, and  $c$  the velocity of light, see fig. 21. The

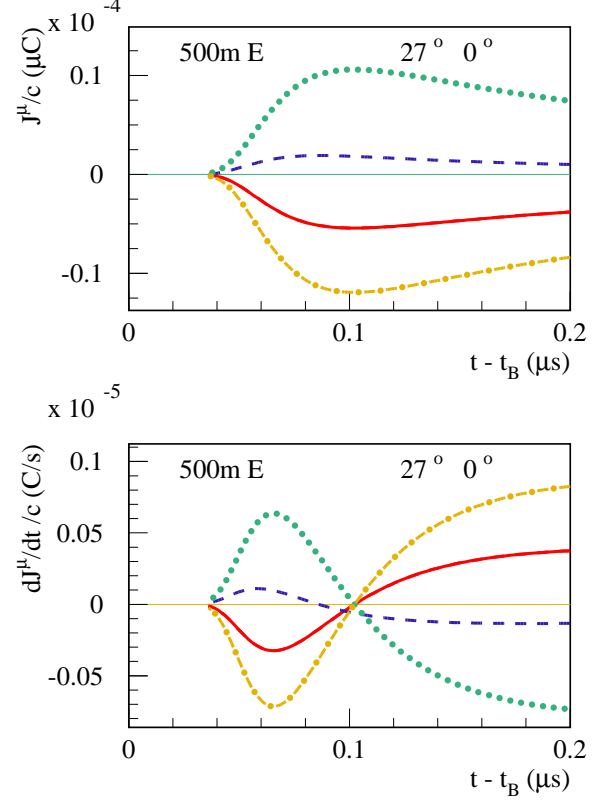


Figure 22: The  $x$ - (full line),  $y$ - (dashed),  $z$ - (dotted), and 0-component (dashed-dotted) of the current  $J$  (top) and their derivatives (bottom) versus the observer time  $t - t_B$ . Here we consider the total current, including the ion contribution. The vector components refer to the Earth frame.

components  $J^x/Nec$  and  $J^y/Nec$  represent the average transverse drift velocity, in units of  $c$ , caused by the magnetic field. Contrary to the case studied in the preceding chapter, we have now a non-vanishing transverse drift and  $J^x/Nec$  is non-zero. The other component  $J^y/Nec$  vanishes because both the shower trajectory and the magnetic field are in the  $y - z$  plane (in the shower frame). The component  $J^z/Nec$  represents the charge excess. The dimensionless quantities  $J^i/Nec$  vary only little with time, corresponding to a transverse drift velocity of 0.04 and a fractional charge excess of -0.2. The small difference compared to the result from the previous chapter is actually due to event by event fluctuations. The time variation of the currents is mainly due to the time variation of  $N$ . For the numerical calculations, also the small time variations of  $J^i/Nec$  are taken into account. Not only the transverse current is non-vanishing, also the dipole moment contributes, see fig. 21.

Expressing the retarded time in terms of the ob-

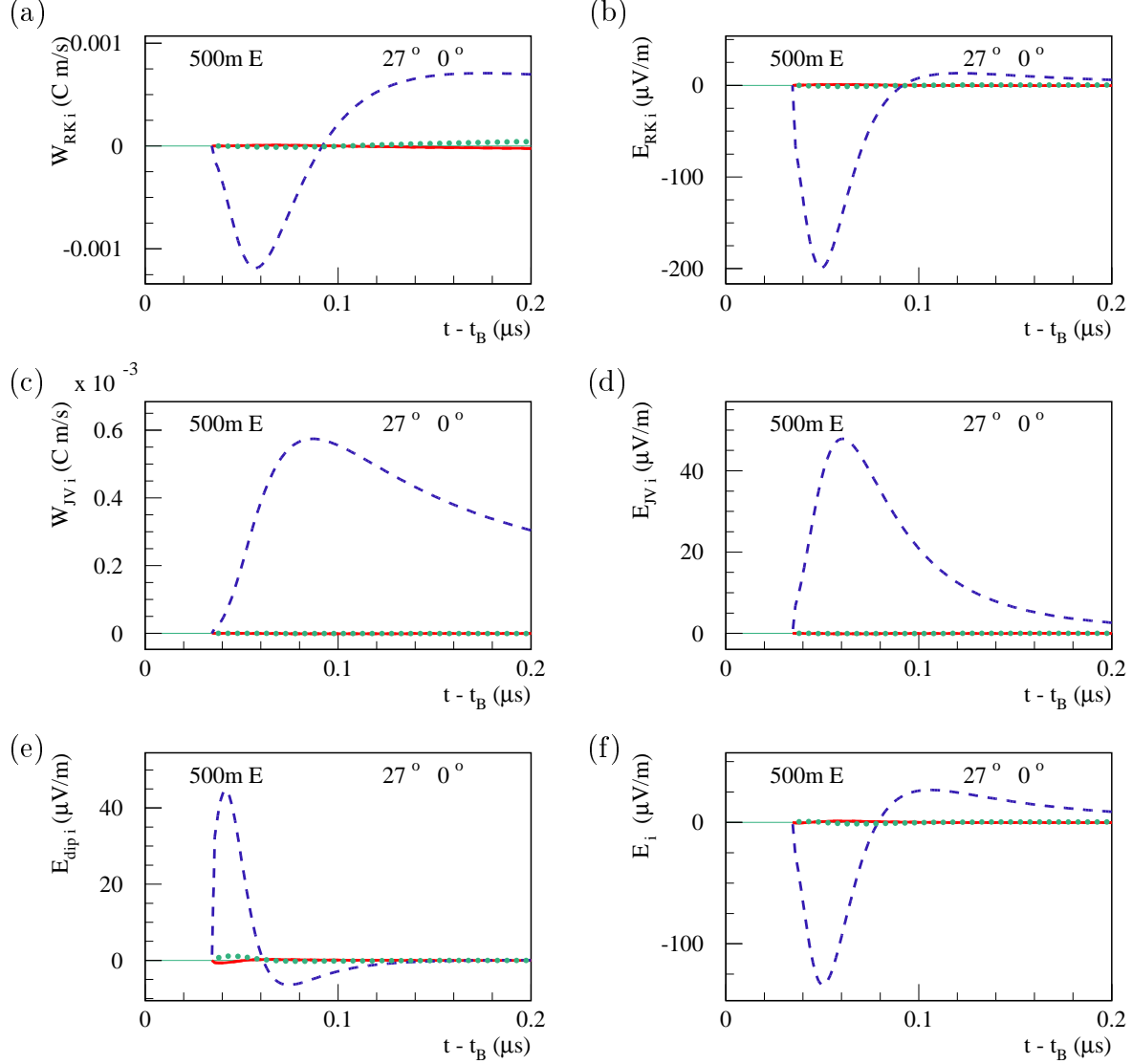


Figure 23: The  $x$ - (full line),  $y$ - (dashed) and  $z$ -component (dotted) of  $\vec{W}_{RK}$  (a),  $\vec{W}_{JV}$  (c), and of the corresponding fields  $\vec{E}_{RK}$  (b),  $\vec{E}_{JV}$  (d), the dipole contribution  $\vec{E}_{dip}$  (e), and the components of the total electric field, with all contributions (f). The vector components refer to the Earth frame.

servation time, the time dependence  $J(t')$  of the current can be expressed as  $J(t^*(t))$  versus the observer time. In fig. 22, we show the components of the current and their derivatives in the Earth frame.

We now discuss the electric fields,

$$\vec{E} = \vec{E}_{dip} + \vec{E}_{RK} + \vec{E}_{JV} = \vec{E}_{dip} + \frac{\vec{W}_{RK}}{D} + \frac{\vec{W}_{JV}}{D}. \quad (68)$$

The three components of the vectors  $\vec{W}$  and the corresponding field contributions, the dipole field components, as well as the three components of the complete field  $\vec{E}$  are shown in fig. 23. The largest contribution is  $\vec{E}_{RK}$ , which has its origin in the time variation of the currents. Also  $\vec{E}_{JV}$  also contributes sig-

nificantly. This contribution is broader but smaller than  $\vec{E}_{RK}$ , and of opposite sign, so the sum of the two gives finally a bipolar field. Compared to the shower parallel to the magnetic field, studied in the previous chapter, both contributions are much bigger, which means that the dominant contribution is due to the transverse current caused by the geomagnetic field. And here, the contribution due to the time variation of this current is by far dominant. But we learn as well that the charge excess contribution cannot be neglected. Also the dipole field contributes significantly, with an opposite sign relative to  $\vec{E}_{RK}$ .



## X. DIFFERENT OBSERVER POSITIONS

In this chapter, we will compare the fields seen by an observer at four different positions: south, east, north, and west of the impact point, always the same distance (500 m). We show in fig. 24 the retarded

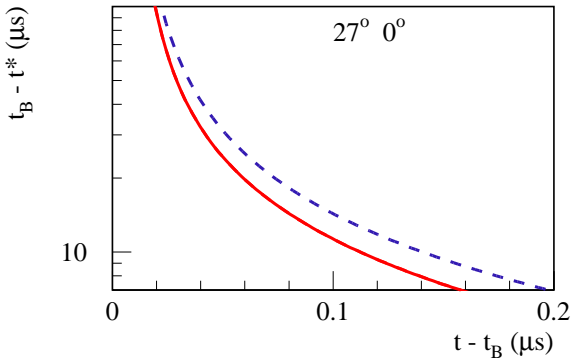


Figure 24: The retarded time expressed via  $t_B - t^*$  versus observer time  $t - t_B$ , for a shower with  $\theta = 27^\circ$ ,  $\psi = 0^\circ$ , seen by observers south (full), or east (dashed) of the point of impact, at a distance of 500 m.

time versus observer time  $t - t_B$ , for our shower with  $\theta = 27^\circ$ ,  $\psi = 0^\circ$ , as seen by different observers. For a given  $b$ , the curves are different for different observers. This fact will help to understand the different widths of the signals seen from the different observers.

We consider first of all a vertical shower ( $\theta = 0^\circ$ ), with the magnetic field artificially turned off. South corresponds to positive  $x$ , east to positive  $y$ . The results are shown in fig. 25. We observe a radial electric field, as expected. The slight deviation of a perfect axial symmetry is due to the fact that the calculation is based on a Monte Carlo generated current, which is of course only approximately symmetric. So even without geo-magnetic field, one observes a sizable field of the order of  $25 \mu\text{V/m}$ .

Also shown in fig. 25 are the fields for a slightly inclined shower, with  $\theta = 27^\circ$ ,  $\psi = 0^\circ$ , still without geomagnetic field. The results are quite similar, we still observe a radial electric field, with respect to the shower axis (with gives a non-zero  $z$ -component in the Earth frame in case of a north or south observer). The signal is also narrower, which is also easy to understand, since in case of non-zero inclination the maximum of the current corresponds to

an earlier retarded time  $t^*$  compared to a vertical shower, and correspondingly the derivative  $dt^*/dt$  is bigger. Therefore a current with a given width in  $t^*$  will be narrower in  $t$ , in case of an inclined shower, leading to a narrower signal.

In fig.26 (upper four plots), we show the results for the same inclined shower, with a realistic geo-magnetic field, but without the dipole contribution. We get in addition to the charge excess contribution (seen in the case without magnetic field) a strong additional contribution perpendicular to the plane defined by shower axis and geo-magnetic field. As discussed earlier, the dominant contribution is  $\vec{E}_{RK}$ , due to the time variation  $K$  of the currents, and here mainly due to the transverse current from the geo-magnetic field. However, seen from the comparison with the  $B = 0$  case, the charge excess is not negligible.

We finally show in fig. 26 (lower four plots) the complete fields for the four observers, including the dipole field. Whereas for the north and the south observers including the dipole field does not change the results, we find for the east and west observers a considerable reduction of the strength due to the dipole contribution.

## XI. CONCLUSION

We introduced a macroscopic calculation of radio emission from air showers initiated by ultra-high energy cosmic rays, based on currents obtained from CONEX Monte Carlo simulations of air showers in a realistic geo-magnetic field. We took into account a realistic index of refraction  $n$ , which varies along the trajectory of the shower.

We demonstrated that in the case of a realistic index of refraction  $n(\vec{y})$  (depending on the space position  $\vec{y}$ ) one can derive expressions for the electric field which are formally equivalent to those for  $n = 1$ , however with a modified definition of the retarded time. One has to take into account the fact that light moves in general on curved trajectories, and that the velocity of light changes along the trajectory. These curves are solutions of differential equations containing  $n(\vec{y})$ . Finding the retarded time amounts to integrating this differential equation, with given boundary conditions. An accurate approximation can be obtained by assuming straight light trajectories. Another delicate point is denominator  $D$  in the expressions for the electric field, which is inversely proportional to the square of the time derivative  $\partial t^*/\partial t$  of the retarded time. This derivative may become singular, and the position of the singularities is strongly affected by the precise value of  $n$ . So even though  $n$  is very close to unity,

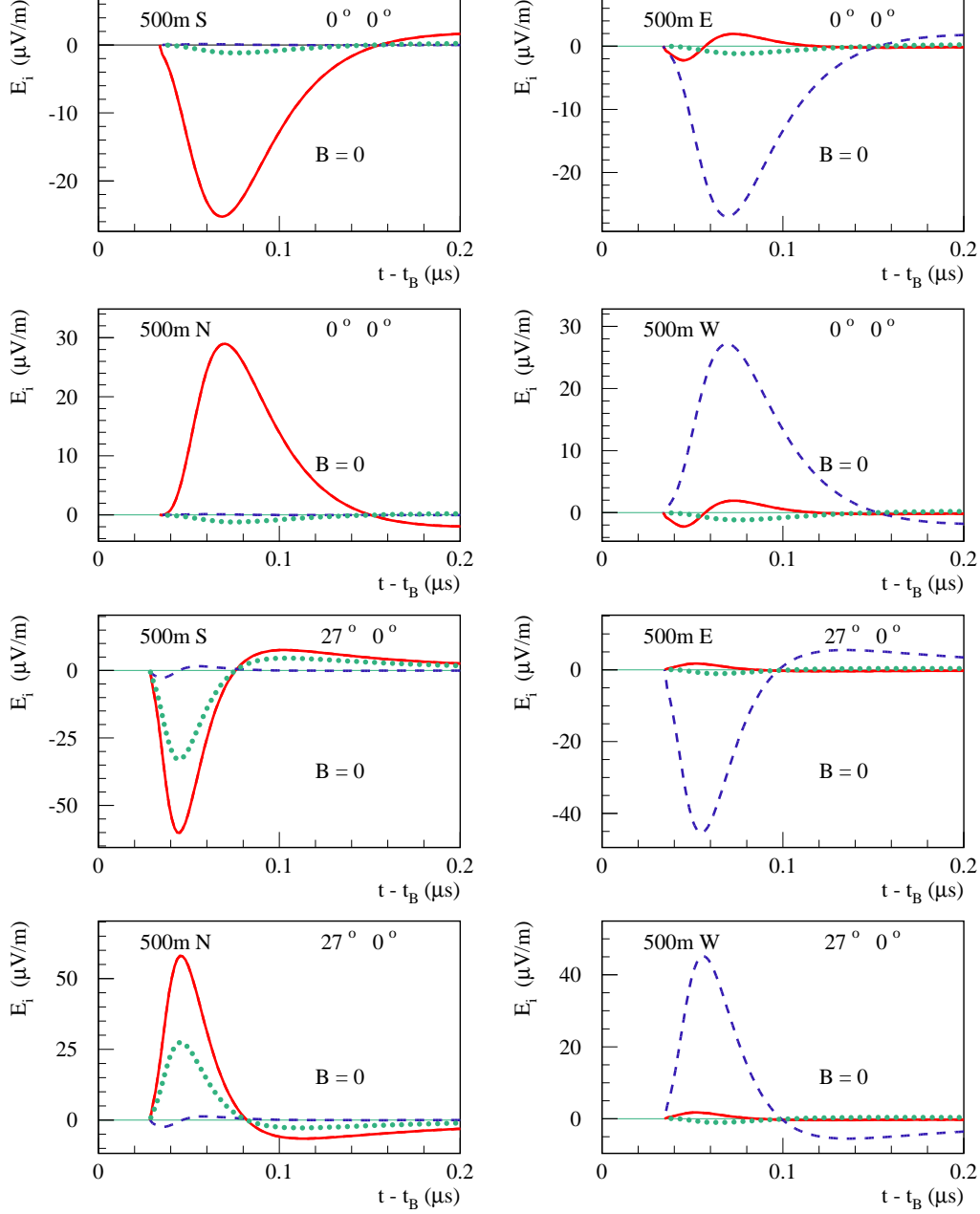


Figure 25: The  $x$ - (full line),  $y$ - (dashed) and  $z$ -component (dotted) of the electric field of a vertical shower (upper four plots) and a shower with  $\theta = 27^\circ$ ,  $\psi = 0^\circ$  (lower four plots), without geo-magnetic field, for four observers 500 m south, east, north, and west of the point of impact. The vector components refer to the Earth frame.

the small deviations from unity are important.

We showed that the electric field can be expressed in terms of the four-vector  $R$  joining the observer's position and the shower, the velocity four-vector  $V$  of the shower, the four-current  $J$ , and the derivative  $K$  of the four-current, as  $\vec{E} = \vec{E}_{\text{dip}} + \vec{E}_{RK} + \vec{E}_{JV} = \vec{E}_{\text{dip}} + (\vec{W}_{RK} + \vec{W}_{JV})/D$  with  $\vec{W}_{AB}$  defined as  $\vec{A}B^0 - A^0\vec{B}$ . The term  $\vec{E}_{JV}$  is zero in case of a longitudinally moving point charge, and non-zero in

case of transverse currents generated by the magnetic field. This contribution therefore vanishes for shower trajectories parallel to the geo-magnetic field, and the contribution increases with increasing angle between shower axis and magnetic field. The most important contribution though is the contribution  $\vec{E}_{RK}$  caused by the time variation  $K$  of the four-current. Here we can identify actually two contributions: one due to time variation of the charge excess,

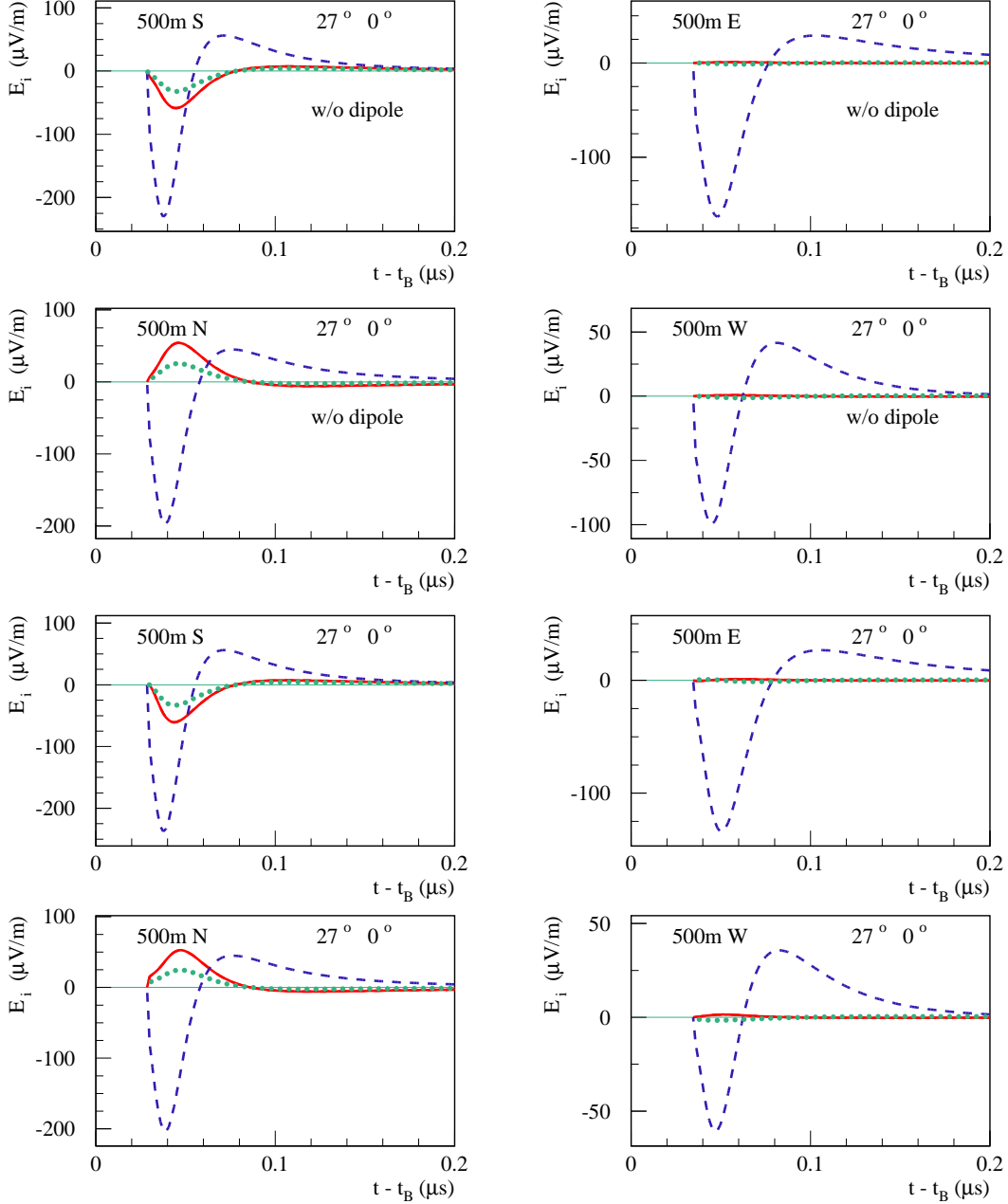


Figure 26: The  $x$ - (full line),  $y$ - (dashed) and  $z$ -component (dotted) of the electric field of a shower with  $\theta = 27^\circ$ ,  $\psi = 0^\circ$ , with the full geo-magnetic field, for four observers south, east, north, and west of the point of impact, at a distance of 500 m. The upper four plots show the fields without the dipole contribution, the lower four plots represent all contributions. The vector components refer to the Earth frame.

which is always present, and an second one due to the time variation of the transverse current due to the geo-magnetic field. This second contribution is only present in case of a non-zero angle between the shower axis and the magnetic field. For the shower we investigated ( $\theta = 27^\circ$ ,  $\psi = 0^\circ$ ), the second contribution is four times larger than the first. The field is thus clearly dominated by the contributions due to the transverse current in the geo-magnetic field, but

the charge excess contribution can not be neglected. Also the dipole field  $\vec{E}_{\text{dip}}$  contributes significantly.

We get in any case a characteristic bipolar signal, reflecting first of all the time dependence of the variation  $K$  of the currents. In case of geo-magnetic contributions this bipolarity is even more pronounced, since here we get an additional contribution  $\vec{E}_{JV}$  whose time signal reflects the time dependence of the current  $J$ , giving therefore a much broader sig-

nal, of opposite sign compared to  $\vec{E}_{RK}$ . The sum is a bipolar signal with two strong pulses.

We emphasize that this bipolarity is in qualitative contrast to the findings of [8, 9, 10, 11, 12], where a microscopic picture has been employed, leading to a single pulse. The fundamental difference is that the time variation of the currents in the macroscopic picture treats in an effective way the creation and disappearance of charges. In a microscopic picture this has to be treated explicitly, otherwise one misses an important part.

### Appendix A: POTENTIAL AND FIELD FROM A POINTLIKE CURRENT

We have

$$j^\beta(x^0, \vec{x}) = \int dx'^0 J^\beta(x'^0) \delta^{(4)}(x - \xi(x'^0)), \quad (\text{A1})$$

with  $x^0 = ct$  and  $\xi_0(x'^0) = x'^0$ . The potential due to the current  $J$  is

$$A^\beta(x) = \mu_0 \int d^4y \frac{1}{2\pi} \theta(x^0 - y^0) \delta((x - y)^2) \times \int dx'^0 J^\beta(x'^0) \delta^{(4)}(y - \xi(x'^0)). \quad (\text{A2})$$

We change  $\int d^4y \dots \int dx'^0 \dots$  into

$$\int dx'^0 \dots \int d^4y \delta^4(y - \xi(x'^0)) \dots, \quad (\text{A3})$$

which gives

$$A^\beta(x) = \frac{\mu_0}{2\pi} \int dx'^0 \theta(x^0 - \xi^0(x'^0)) \times \delta((x - \xi(x'^0))^2) J^\beta(x'^0). \quad (\text{A4})$$

Using  $R = x - \xi(x'^0)$ , we have

$$A^\beta(x) = \frac{\mu_0}{2\pi} \int dx'^0 \theta(x^0 - \xi^0(x'^0)) \delta(R^2) J^\beta(x'^0). \quad (\text{A5})$$

Using

$$\delta(R^2) = \frac{\delta(x'^0 - \tilde{x}^0)}{|(dR^2/dx'^0)_{x'^0=\tilde{x}^0}|}, \quad (\text{A6})$$

with  $x'^0$  being the root of  $R^2$  (supposing there is only one), and

$$\frac{dR^2}{dx'^0} = 2R \frac{dR}{dx'^0} = -2RV,$$

with  $V = d\xi/dx'^0$ , we get for  $x_0 \neq \xi_0(x'^0)$

$$A^\beta(x) = \frac{\mu_0}{4\pi} \frac{J^\beta}{|RV|}, \quad (\text{A7})$$

with all quantities considered at the retarded time  $x'^0$ . The electric field is given as

$$E^i = c(\partial^i A^0 - \partial^0 A^i). \quad (\text{A8})$$

We have

$$\partial^\alpha A^\beta(x) = \frac{\mu_0}{4\pi} \partial^\alpha \frac{J^\beta}{|RV|}. \quad (\text{A9})$$

We have

$$\partial^\alpha \frac{J^\beta}{|RV|} = \frac{dJ^\beta/d\tilde{x}^0}{|RV|} \partial^\alpha x'^0 - \frac{J^\beta}{RV|RV|} \partial^\alpha \{RV\}. \quad (\text{A10})$$

The derivative of  $RV$  is

$$\partial^\alpha \{RV\} = V^\alpha - VV \partial^\alpha x'^0. \quad (\text{A11})$$

From  $R^2 = 0$  we conclude

$$\partial^\alpha R^2 = 2R^\alpha - 2RV \partial^\alpha x'^0 = 0, \quad (\text{A12})$$

so

$$\partial^\alpha x'^0 = \frac{R^\alpha}{RV}. \quad (\text{A13})$$

Putting all together, we obtain

$$\partial^\alpha A^\beta(x) = \frac{\mu_0}{4\pi} \frac{L^{\alpha\beta}}{|RV|^3}, \quad (\text{A14})$$

with

$$L^{\alpha\beta} = RV R^\alpha \dot{J}^\beta - RV J^\beta V^\alpha + VV R^\alpha J^\beta. \quad (\text{A15})$$

where the ‘‘dot’’ means derivative with respect to  $x'^0$ . The electric field is then

$$E^i(x) = \frac{1}{4\pi\epsilon_0 c} \frac{L^{i0} - L^{0i}}{|RV|^3}, \quad (\text{A16})$$

with  $n$  being the index of refraction at the observer position.

### Appendix B: CURRENTS FROM AIR SHOWER SIMULATIONS

We compute the current by using the CONEX shower simulation program, as

$$\vec{J} = \sum_{\text{positrons } i} e\vec{v}_i - \sum_{\text{electrons } j} e\vec{v}_j, \quad (\text{B1})$$

considering all electrons and positrons present at a given time. With  $t_0$  being the creation time of a particle, its velocity some time later can be written as

$$\vec{v}(t) = \vec{v}_\parallel(t_0) + |\vec{v}_\perp(t_0)|(\vec{e}_1 \cos \omega t + \vec{e}_2 \sin \omega t), \quad (\text{B2})$$

where  $\vec{v}_{\parallel}$  and  $\vec{v}_{\perp}$  are the velocity components parallel and orthogonal to the magnetic field,  $\omega = \pm eB/\gamma m$ , and where  $\{\vec{e}_i\}$  is a system of orthonormal vectors, defined via

$$\vec{e}_3 = \vec{B}/|\vec{B}|, \quad \vec{e}_1 = \vec{v}_{\perp}(t_0)/|\vec{v}_{\perp}(t_0)|, \quad \vec{e}_2 = \vec{e}_1 \times \vec{e}_3. \quad (\text{B3})$$

We define a ‘‘shower frame’’  $\{A, \vec{u}_x, \vec{u}_y, \vec{u}_z\}$ , where the vectors can be expressed with respect to the Earth frame basis as

$$\vec{u}_x = \begin{pmatrix} 0 \\ 1 \\ 0 \end{pmatrix}, \quad \vec{u}_y = \begin{pmatrix} \cos \theta \\ 0 \\ \sin \theta \end{pmatrix}, \quad \vec{u}_z = \begin{pmatrix} \sin \theta \\ 0 \\ -\cos \theta \end{pmatrix}. \quad (\text{B4})$$

The vector  $\vec{u}_z$  is parallel to the shower axis ( $z$  is the longitudinal shower variable). Again with respect to the Earth frame basis, the magnetic field may be written as

$$\vec{B} = B \begin{pmatrix} \sin \alpha \cos \varphi \\ \sin \alpha \sin \varphi \\ \cos \alpha \end{pmatrix}, \quad (\text{B5})$$

where  $\alpha$  is the angle between  $\vec{B}$  and the  $\vec{u}_z$ , and  $\varphi$  the angle between the shower plane and the plane containing  $\vec{B}$  and the vertical axis. Computing

$\vec{B}\vec{u}_{x,y,z}$ , we obtain  $\vec{B}$  in the shower coordinate system, and as well  $\vec{e}_3 = \vec{B}/B$ ,

$$\vec{e}_3 = \begin{pmatrix} \sin \alpha \sin \varphi \\ \sin \alpha \cos \varphi \cos \theta + \cos \alpha \sin \theta \\ \sin \alpha \cos \varphi \sin \theta - \cos \alpha \cos \theta \end{pmatrix}. \quad (\text{B6})$$

Then

$$v_{\parallel} = \vec{v} \cdot \vec{e}_3, \quad \vec{v}_{\parallel} = v_{\parallel} \vec{e}_3, \quad , \quad \vec{v}_{\perp} = \vec{v} - \vec{v}_{\parallel}, \quad v_{\perp} = |\vec{v}_{\perp}|, \quad (\text{B7})$$

and

$$\vec{e}_1 = \vec{v}_{\perp}/v_{\perp}, \quad \vec{e}_2 = \vec{e}_1 \times \vec{e}_3. \quad (\text{B8})$$

Now we know the components of the vectors  $\vec{e}_i$  in the shower frame, which allows us to evaluate eq. B2 and determine the components  $J^i$  of the current in the shower frame. We finally obtain easily the components of the currents with respect to the Earth frame basis as

$$\vec{J} = J^x \vec{u}_x + J^y \vec{u}_y + J^z \vec{u}_z, \quad (\text{B9})$$

and its derivatives.

- 
- [1] H. Falcke, et al., Nature **435**, 313 (2005).  
[2] W. D. Apel, et al., Astropart. Physics **26**, 332 (2006).  
[3] D. Ardouin, et al., Astropart. Physics **26**, 341 (2006).  
[4] H. R. Allan, Prog. in Element. part. and Cos. Ray Phys. **10**, 171 (1971).  
[5] F.D. Kahn and I.Lerche, Proc. Royal Soc. London **A289**, 206 (1966).  
[6] N.A. Porter, C.D. Long, B. McBreen, D.J.B Murnaghan and T.C. Weekes, Phys. Lett. **19**, 415 (1965).  
[7] J. V. Jelley et al., Nature **205**, 327 (1965).  
[8] T. Huege, H. Falcke, Astronomy & Astrophysics **412**, 19 (2003).  
[9] H. Falcke and P. Gorham, Astropart. Phys. **19**, 477 (2003).  
[10] D.A. Suprun, P.W. Gorham, J.L. Rosner, Astropart. Phys. **20**, 157 (2003).  
[11] T. Huege, H. Falcke, Astronomy & Astrophysics **430**, 779 (2005); T. Huege, H. Falcke, Astropart. Phys. **24**, 116 (2005).  
[12] T. Huege, R. Ulrich, and R. Engel, Astropart. Phys. **27**, 392 (2007)  
[13] O. Scholten, K. Werner, F. Rusydi, arXiv:0709.2872, accepted for publication in Astropart. Phys.  
[14] G. Bossard, H.J. Drescher, N.N. Kalmykov, S. Ostapchenko, A.I. Pavlov, T. Pierog, E.A. Vishnevskaya, and K. Werner, Phys. Rev. **D63**, 054030, (2001)  
[15] T. Bergmann R. Engel, D. Heck, N.N. Kalmykov, Sergey Ostapchenko, T. Pierog, T. Thouw, and K. Werner, Astropart. Phys. **26**, 420 (2007)